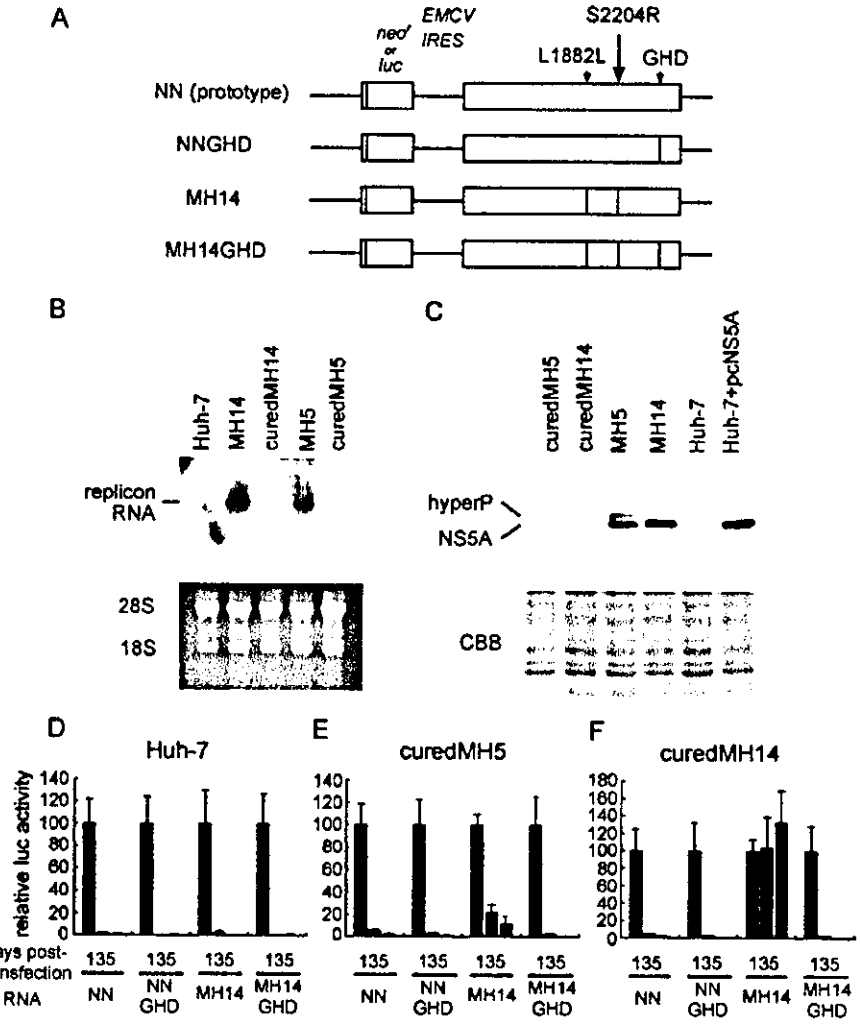

Fig. 1. Constructions and cells used in this study. (A) Schematic representation of the subgenomic replicon RNA constructs. The prototype NN RNA was used for transfection to obtain subgenomic replicon cell lines, including MH5 and MH14. NNGHD denotes polymerase-defective mutant, in which the catalytic GDD motif of the NS5B polymerase was substituted to the inactive GHD motif, and was used as a negative control. MH14 RNA carries two mutations, which were found in the replicon RNA in MH14 subgenomic replicon cells. MH14GHD is a negative control for the MH14 RNA. The ORFs are depicted as open boxes. The locations of the mutations introduced into the viral proteins are indicated by vertical lines. (B) Northern blot analysis of total RNA extracted from replicon cells. RNA from Huh-7, MH14, curedMH14, MH5, or curedMH5 cells was electrophoresed on denaturing agarose gels, blotted, and probed with an HCV RNA (upper panel). As an internal control, the ethidium bromide-staining pattern of 28S and 18S ribosomal RNA is shown (lower panel). (C) Western blot analysis of NS5A protein expressed in Huh-7, MH14, curedMH14, MH5, or curedMH5 cells (upper panel). As a control, wild-type NS5A protein was exogenously produced in Huh-7 cells from an expression plasmid (Huh-7 + pcNS5A). The position of the hyper-phosphorylated form of the protein is designated HyperP. As an internal control, the Coomassie brilliant blue (CBB) staining pattern of the same blot is shown (lower panel). (D–F) Replication of replicon RNAs with mutations in Huh-7 cells or its derivatives. Huh-7 (D), curedMH5 (E), or curedMH14 (F) cells were transfected with replicon RNA constructs containing the luciferase gene (depicted in A). Luciferase activity was measured at 1, 3, and 5 days after transfection. Each bar represents the mean and SD of three independent transfections.

the effect of TGF-β on luciferase expression and activity, the pCMV-Luc, in which the firefly luciferase gene is driven under the control of the CMV promoter, was used in Fig. 2C. While TGF-β treatment repressed the luciferase expression from replicon (Fig. 2B), we found that the cytokine enhanced the luciferase expression from the CMV promoter (Fig. 2C), provably because of the activation of transcriptional factors (Derynck and Zhang, 2003; Miyazono et al., 2000).

TGF-β is a multifunctional cytokine that exerts a range of biological activities, including cell growth inhibition (Derynck and Zhang, 2003; Miyazono et al., 2000). When exposed to TGF-β, cells generally arrest in the G(1)/S phase of the cell cycle. We, therefore, examined cell growth of curedMH14 cells (Fig. 2D). As expected, the growth of curedMH14 cells was partially inhibited by cytokine treatment (Fig. 2D, open circle). As assessed by FACS, administration of TGF-β for 2–3 days resulted in G(1)/S-arrest, while a 1-day treatment had no effect on cell cycle (Fig. 2E).

Fifty percent suppression of luciferase activity, after 3 days of treatment, was observed in the presence of

approximately 0.1 ng/ml TGF-β (Fig. 2F). Cell growth started to be suppressed at similar concentrations (Fig. 2G).

Smad-dependent suppression of HCV replicon

The cellular effects of TGF-β are mediated by both type I and type II serine/threonine kinase receptors. Receptor ligation is followed by the activation of both the canonical Smad and the MAPK signaling pathways, which include p38 MAPK, JNK, and ERK (Derynck and Zhang, 2003; Miyazono et al., 2000). To clarify the signaling pathways crucial for the suppression of HCV replication, we utilized two constitutive active receptors. One constitutively active TGF-β type-I receptor, TβR-I(T/D), evokes both Smad and

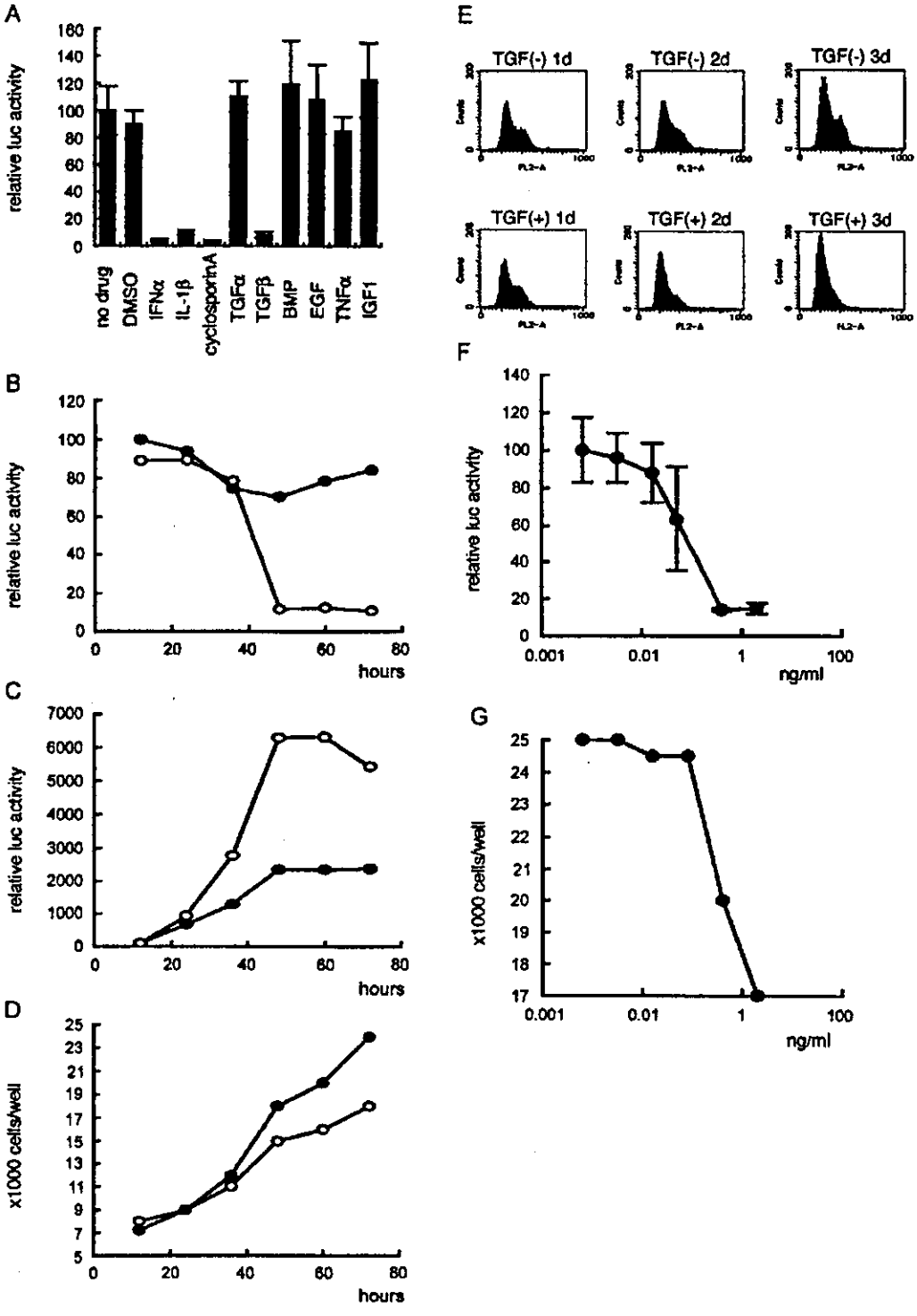

MAPK pathways, even in the absence of the TGF-β ligand (Imamura et al., 1997). The other constitutively active type-I receptor, TβR-ImL45(T/D), only activates the MAPK pathways, lacking the ability to excite Smad signaling (Yu et al., 2002). Three days after transfection of curedMH14 cells with the combination of the luciferase-replicon (LMH14) RNA and the TβR-I(T/D) expression plasmid, luciferase activity was reduced to 37% of the control levels, even in the absence of TGF-β (Fig. 3A). In contrast, co-transfection with TβR-ImL45(T/D) produces 71% of the control levels of luciferase activity, suggesting that the second constitutively active receptor had little effect on HCV replication (Fig. 3A). As summarized in Figs. 4B and C, the TβR-I(T/D) receptor likely activated transcription from promoters containing either AP-1-or Smad-responsive elements, while the TβR-ImL45(T/D) evoked transcription from the AP-1-dependent promoter alone. These data serve as evidence that the antiviral activity of TGF-β is dependent on Smad signaling.

Upon TGF-β stimulation, R-Smads specific for this cytokine, Smad2 and Smad3, are activated, forming complexes with the Co-Smad, Smad4, to activate transcription from the corresponding promoters. As co-expression of Smad2 with Smad4 or Smad3 with Smad4 mimics the effects of TGF-β stimulation (Yingling et al., 1997), we tested if such the co-expression of these molecules would also suppress HCV replicon production. Transfection of either Smad2/4 or Smad3/4 reduced the luciferase activity to 16% or 13%, respectively, even in the absence of TGF-β (Fig. 3A). Expression of an inhibitory-Smad (I-Smad), Smad7, which inhibits TGF-β mediated Smad signaling (Derynck and Zhang, 2003), only modestly reduced (81% of the control) the luciferase activity (Fig. 3A). The enhancement of transcription from AP-1-responsive (Fig. 3C), as well as TGF-β-responsive (Fig. 3B), promoters by co-transfection of either Smad2/4 or Smad3/4 was expected, as Smad4 itself has been reported to elicit transcription from AP-1 binding site-containing promoters (Liberati et al., 1999; Yingling et al., 1997).

To verify whether the Smad but not MAPK signaling is crucial for the suppression of HCV replicon by TGF-β,we used several specific MAPK inhibitors to examine if the antiviral effect of TGF-β is associated with the activation of specific MAPKs. The addition of inhibitors of ERK, p38, or JNK, U0126, SB20350, or dexamethasone, respectively, did not cancel TGF-β suppression of luciferase activity (Fig. 4A), despite effective inhibition of kinase activity by the inhibitors (Figs. 4B–D). The phosphorylation of ERK by TGF-β was not observed under these conditions (Fig. 4B), as ERK was already activated by growth factors contained within the bovine serum supplementing the culture medium.

Suppression of G418-resistant replicon by TGF-β

We then investigated the effect of TGF-β on G418-resistant replicon RNA or protein levels. MH14, G418-resistant subgenomic replicon cells, were treated with IFN-α, TGF-β, or BMP-4. BMP-4 was used here because it is a member of TGF-β superfamily cytokines and it does not induce inhibition of cell proliferation at least in Huh-7 cells. Total RNA and protein were collected at various time points. RNAs were subjected to Real-Time RT-PCR (Fig. 5A) or Northern blotting (Fig. 5B), while proteins were examined by Western blotting (Fig. 5C). Replicon RNA levels gradually decreased following treatment with 2 ng/ml TGF-β to 0.6% of the levels observed in mock-treated samples on the 7th day. This inhibition was similar to that seen following treatment with 100 IU/ml IFN-α. The NS5A protein was virtually undetectable by the 5th day after transfection (Fig. 5C). The suppressive effect of TGF-β on viral protein production was also observed by indirect immunofluorescence (not shown).

Because the replicon RNA of MH14 cells has the EMCV IRES to produce NS proteins, one could not deny the possibility that the EMCV IRES might cause the inhibition by TGF-β. Therefore, we next used full-genome replicon cell line SNC#2 (Fig. 6), which has the HCV IRES instead of the EMCV IRES, and tested if TGF-β would affect the replication. As shown in Fig. 6B, replicon RNA in SNC#2 cells treated with TGF-β decreased clearly while BMP-4 did not suppress the RNA levels.

Simultaneous suppression of viral RNA replication and protein synthesis by TGF-β

The suppression of HCV replication by TGF-β treatment was associated with the inhibition of cell growth. We examined the kinetics of the suppression of HCV replication

Fig. 2. Suppression of luciferase-replicon by TGF-β. (A) curedMH14 cells transfected with the luciferase-replicon RNA construct (LMH14), were administered with DMSO (0.1%), IFN-α (100 IU/ml), IL-1β (10 ng/ml), cyclosporin A (1 μg/ml), TGF-α (1 ng/ml), TGF-β (2 ng/ml), BMP-4 (10 ng/ml), mEGF (100 ng/ml), TNF-α (10 ng/ml), or IGF-1 (1 ng/ml). Three days later, cellular luciferase activity was measured. Bars represent the mean and SD of three independent experiments. (B) curedMH14 cells transfected with LMH14 luciferase-replicon RNA construct were mock-treated (black circle) or treated with TGF-β (2 ng/ml, white circle). At the indicated times, cells were harvested for determination of luciferase activity. The activity was normalized to cell number. (C) In parallel with the experiments in Fig. 3B, cells transfected with pCMV-Luc were mock-treated (black circle) or treated with TGF-β (2 ng/ml, white circle). At the indicated times, cells were harvested for determination of luciferase activity. The activity was normalized to cell number. (D) In parallel with the experiments in Fig. 3B, cells were mock-treated (black circle) or treated with TGF-β (2 ng/ml, white circle). Cell numbers were counted at the indicated time points. (E) Flow cytometric analysis of cell cycle progressing in curedMH14 cells transfected with the S2204R luciferase-replicon RNA construct. Cells were incubated in the presence or absence of TGF-β (2 ng/ml) for 1, 2, or 3 days. The DNA content of these cells was analyzed as described in Materials and methods. Dose-dependence of luciferase-replicon (F) and cell growth inhibition (G). curedMH14 cells transfected with the LMH14 luciferase-replicon RNA construct were treated with varying concentrations of TGF-β for 3 days. Luciferase activity (F) and cell number (G) were subsequently determined. The luciferase activity was normalized to cell number and shown with the SD value of three experiments in F.

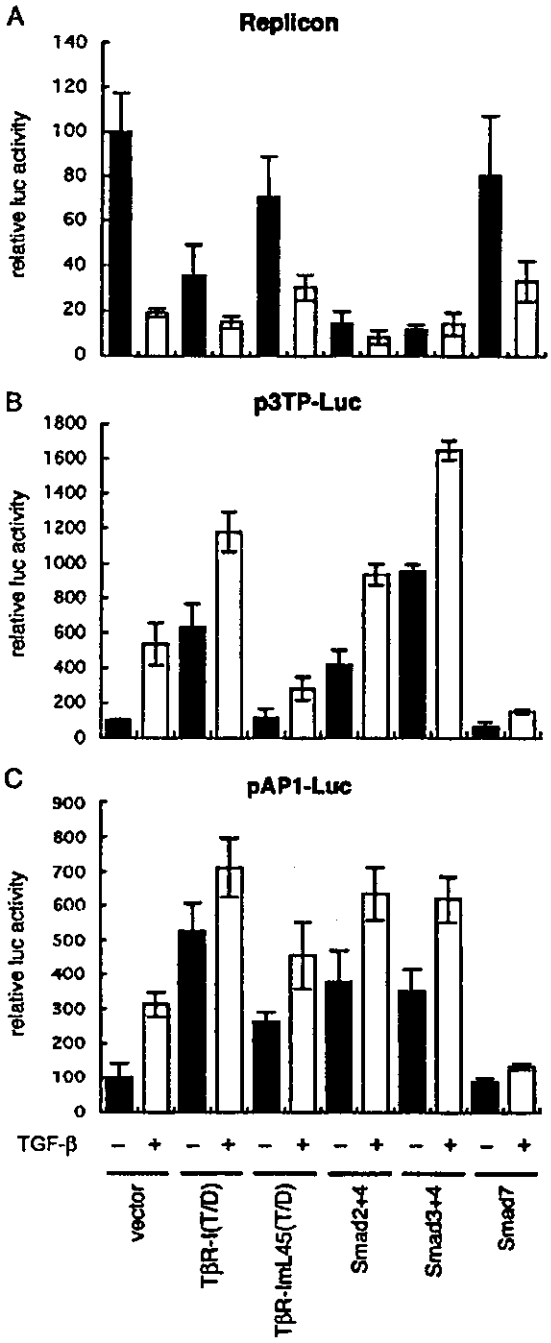

Fig. 3. Expression of TGF-β signaling-related proteins affected HCV replicon. curedMH14 cells were transfected with the expression plasmid designated below panel C together with (A) the luciferase-replicon construct with the mutations (LMH14), (B) p3TP-Luc, to monitor Smad-dependent transcription, or (C) pAP1-Luc, used to monitor AP-1-dependent transcription. Four hours after transfection, TGF-β (2 ng/ml) was added. Cells were incubated with or without the cytokine for 3 days (A) or 12 h (B, C) and then cellular luciferase activity was measured. The luciferase activity in A was normalized to cell number and then, the mean and SD value of three transfections are shown.

by examining viral RNA and protein synthesis rates at various times after the inoculation of replicon cells with the cytokine (Fig. 7). Aphidicolin and IFN-α were used as controls. The inhibition of viral protein synthesis by 100 IU/ml IFN-α began 12 h after treatment, while viral RNA synthesis was not affected until 24 h after cytokine addition. These results suggest that IFN-α first represses protein synthesis, thereby blocking RNA replication. In contrast, both aphidicolin and TGF-β inhibited protein synthesis and RNA replication concurrently, by 48 h after treatment. As both aphidicolin and TGF-β have growth inhibitory effects on cells, it is likely that both prevent HCV replicon in similar manners.

Anti-HCV activity of TGF-β was not mediated by IFN-induced signaling pathway

Although the antiviral activity of TGF-β was dependent on Smad signaling, the possibility remains that TGF-β may exert an antiviral activity via the same mechanisms as IFN-α and -γ. The binding of IFN-α or -γ to cellular receptors activates the JAK tyrosine kinase, which in turn phosphorylates effector Stat proteins. These proteins stimulate transcription from promoters with the specific sequences, ISRE or GAS, respectively. We prepared reporter plasmids that produce firefly luciferase following IFN-α or -γ stimulation by placing the gene under the control of a promoter containing either ISRE or GAS sequence. While 100 IU/ml IFN-α stimulation enhanced transcription from the ISRE-promoter 3.5-fold, enhancement of promoter activity was not observed following TGF-β treatment (Fig. 8A). The addition of 1000 IU/ml IFN-γ activated the GAS-dependent promoter by 5.8-fold, while TGF-β had little effect (Fig. 8B). The results suggest that TGF-β exerts its antiviral activity in a manner independent of IFN signaling.

Discussion

First, we have developed an efficient HCV subgenomic replicon system in this study. When maintained in cells, HCV replicon RNA often acquires cell culture-adaptive mutations. We found that the replicon RNA in MH14 cells carries two mutations, L1882L and S2204R. Among them, the S2204R, but not the L1882L, mutation was necessary and sufficient for the high efficiency (not shown). Although the mechanism by which the adaptive mutation produce high replication efficiency is not known, the interaction of the NS5A protein with a co-factor, such as hVAP-A (Gao et al., 2004; Tu et al., 1999), might explain the phenomenon.

As cytokines can play major roles in pathogenetic process during the courses of viral diseases, the relationships between viruses and cytokines, such as TGF-β, are of great importance. In this study, we found that TGF-β inhibits viral RNA replication and protein expression in the HCV replicon system.

The mechanism by which IFN-α suppresses HCV replicon is not well understood. Here, we showed that

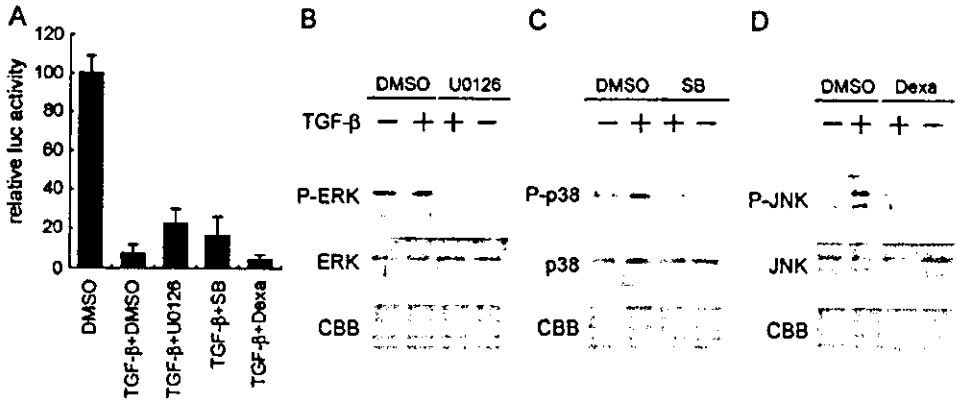

Fig. 4. Effect of MAPKs on the HCV replicon. (A) curedMH14 cells transfected with the luciferase-replicon construct (LMH14) were treated with DMSO, TGF-β (2 ng/ml) plus DMSO, or TGF-β (2 ng/ml) with either U0126 (3 μM), SB203580 (30 μM), or dexamethasone (1 μM). Inhibitors were added 1 h prior to the addition of TGF-β . After a 3-day treatment, cellular luciferase activity was measured. The mean and SD of three independent transfections are depicted after normalization to cell number. (B–D) The effect of inhibitors on the phosphorylation of ERK (B), p38MAPK (C), and JNK (D). Western blotting examined the phosphorylation of these molecules in cells treated with or without the designated reagents. The upper panels depict phosphorylated MAPKs, while the middle panels display the total amount of the MAPKs. CBB staining pattern of the same blot is used as a loading control (lower panel).

IFN-α repressed protein synthesis first, then suppressed RNA replication of the HCV replicon (Fig. 7). These data seem to support the previous report (Guo et al., 2004) and may aid our understanding of the suppression mechanism by IFN-α. IFN-α might suppress HCV translation trough the La (Shimazaki et al., 2002)-, ISG56 (Sumpter et al., 2004) or PKR (Wang et al., 2003)-dependent manner.

In contrast, either aphidicolin or TGF-β simultaneously inhibited both protein synthesis. and RNA replication from the replicon de novo (Fig. 7). While the mechanism of simultaneous suppression by aphidicolin or TGF-β remains unknown, both reagents arrest cell cycle progression at G(1)/S, suggesting a common target in the repression of HCV replicon expression. Recently, Scholle et al. (2004) reported that the replication of the HCV replicon RNA depends on host cell growth. Our results clearly correspond with that report, in which viral RNA levels remained unchanged during a 24-h period of cell cycle arrest followed by drops by 48 h.

It has been demonstrated that cell cycle arrest by TGF-β is mainly caused in the Smad pathway-dependent manner and the MAPK signaling serves as an accessory modifier of the arrest (Ten Dijke et al., 2002). Therefore, our result is convincing in that Smad, but not the MAPK pathway, played an essential role in the suppression of HCV replication.

Broadly speaking, serological investigations of HCV in chronically infected patients imply an inverse relationship between viral RNA load and TGF-β levels. Increased TGF-β expression significantly correlates with the degree of hepatic fibrosis (Calabrese et al., 2003; Nelson et al., 1997). A 3-year follow-up study demonstrated that TGF-β levels were elevated in patients with fibrosis that was

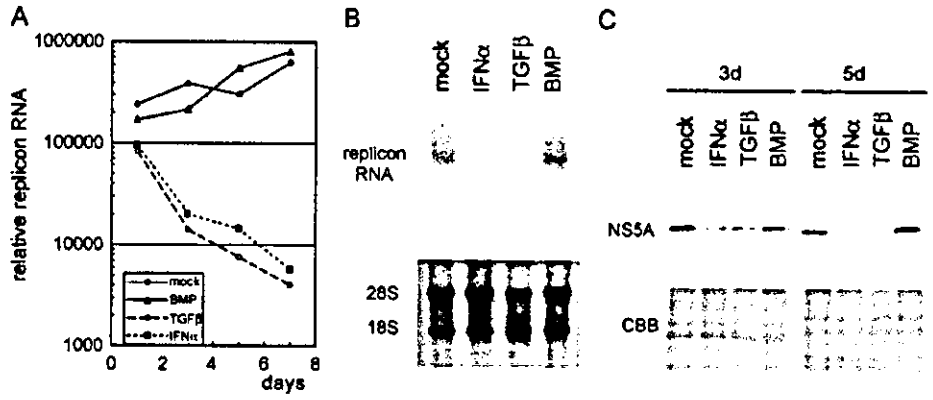

Fig. 5. Suppression of G418-resistant subgenomic replicon by TGF-β. (A) MH14, a G418-resistant subgenomic replicon cell line, was mock-treated or treated with BMP-4 (10 ng/ml), TGF-β (2 ng/ml), or IFN-α (100 IU/ml) for 1, 3, 5, or 7 days. Following the extraction of total RNA, the quantity of HCV replicon RNA was determined by real-time RT-PCR analysis. (B) Total RNA was also subjected to Northern blot analysis (upper panel). The ethidium bromide-staining pattern of ribosomal RNA is shown as an internal control (lower panel). (C) Total protein from cells prepared as above was harvested after either 3 or 5 days of cytokine treatment. Western blot analysis was performed using an antibody against NS5A. CBB staining pattern of the same blot is shown as a loading control (lower panel).

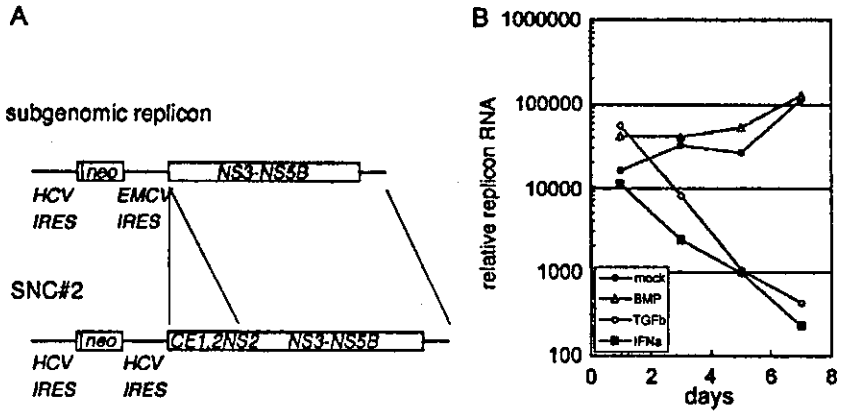

Fig. 6. Suppression of G418-resistant replicon without EMCV IRES by TGF-β. (A) Schematic representation of an RNA construct in typical subgenomic replicon cells (upper) and that in SNC#2 replicon cells (lower). RNA in SNC#2 carries the sequence for the whole HCV ORFs, driven by the HCV IRES instead of the EMCV IRES. The ORFs are depicted as open boxes. (B) SNC#2 cells were mock-treated or treated with BMP-4 (10 ng/ml), TGF-β (2 ng/ml), or IFN-α (100 IU/ml) for 1, 3, 5, or 7 days. Following the extraction of total RNA, the quantity of HCV replicon RNA was determined by real-time RT-PCR analysis.

increasing in severity (Neuman et al., 2002), which correlated with lower levels of viremia in patients than those with less progressed fibrosis (Adinolfi et al., 2001). These reports suggest that the presence of TGF-β, which may be induced by HCV core protein (Taniguchi et al., 2004), has a suppressive influence on viral RNA load. Gewaltig et al. (2002) demonstrated that polymorphisms in the TGF-β gene were associated with progression of HCV-induced liver fibrosis, suggesting again that the cytokine and the cytokine signaling have a certain influence on the virus.

The precise molecular mechanism of the anti-HCV activity of TGF-β remains to be clarified. Additional studies, including clinical studies, may reveal a novel mechanism of HCV replication regulation, potentially providing a target for novel anti-HCV therapies in the future.

Materials and methods

Cell culture, antibodies, and reagents

Huh-7, curedMH5, and curedMH14 cells were maintained in Dulbecco's modified Eagle medium (Gibco BRL) supplemented with 10% fetal bovine serum, 100 units/ml nonessential amino acids (Invitrogen), and 100 μg/ml of both penicillin and streptomycin sulfate (Invitrogen). MH5, MH14, and SNC#2 replicon cells were cultured in the above medium supplemented with 300 μg/ml G418 (Geneticin, Invitrogen). Cured cells were prepared by treating cells with 5000 IU/ml of IFN-α for 2 weeks. Absence of replicon RNA and viral proteins was checked by Northern blotting, Western blotting, and RT-PCR.

Rabbit antisera raised against p38, JNK, ERK, and phospho-ERK were purchased from Cell Signaling Tech-

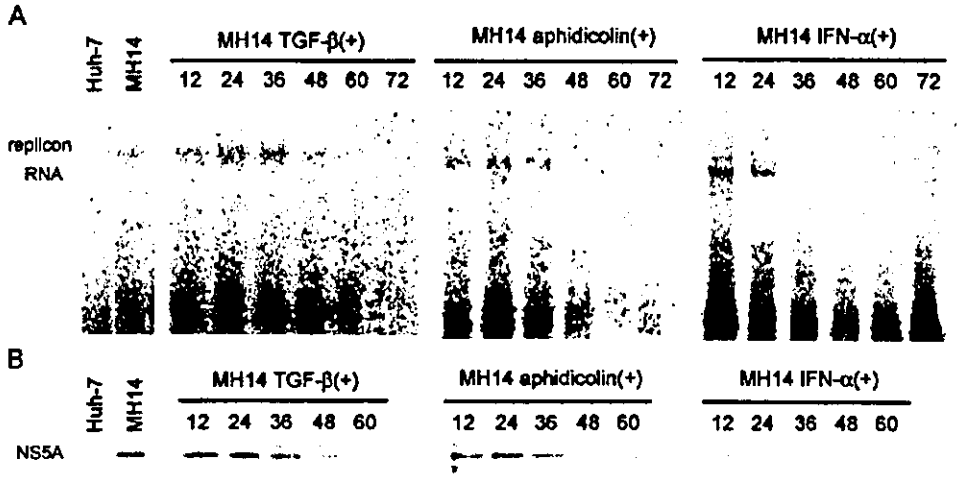

Fig. 7. Simultaneous suppression of viral RNA replication and protein synthesis by TGF-β. (A, B) MH14, a G418-resistant subgenomic replicon cell line, was mock-treated or treated with TGF-β (2 ng/ml), aphidicolin (5 μg/ml), or IFN-α (100 IU/ml) for 12, 24, 36, 48, 60, or 72 h. Cells were then subjected to semi-intact replication assay (A) or [^{35}S]-methionine metabolic labeling and immunoprecipitation using an anti-NS5A antibody (B) as described in Materials and methods.

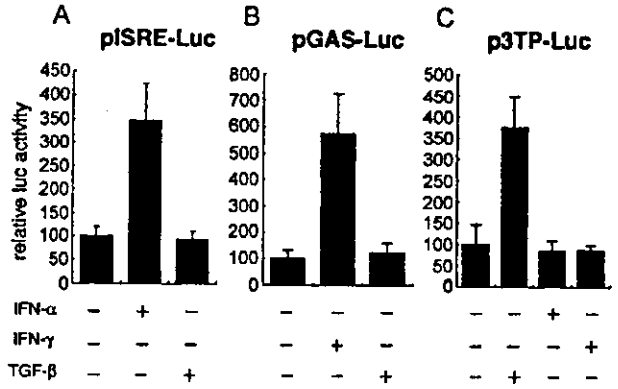

Fig. 8. TGF-β exerts an anti-HCV activity independent of the signal transduction pathway activated by IFN-α or -γ. curedMH14 cells were transfected with either pISRE-Luc (A), pGAS-Luc (B) or p3TP-Luc (C) and treated with TGF-β (2 ng/ml), IFN- (100 IU/ml), or IFN-γ (1000 IU/ml). Luciferase activities were measured 12 h after transfection. Data represent the means and SD values of relative luciferase activities in three independent experiments.

nology. Mouse antibodies specific for phospho-p38 and phospho-JNK were acquired from BD Biosciences and SIGMA, respectively. Horseradish peroxidase-conjugated goat antibodies to mouse and rabbit IgG were procured from Amersham Biosciences. TGF-β, BMP-4, and SB203580 were obtained commercially from Calbiochem. U0126 and Dexamethasone were purchased from SIGMA.

Northern and Western blot analysis

RNA was extracted from cells using Sepasol RNAI super reagent (Nacalai Tesque, Kyoto, Japan) according to the manufacturer's protocol. Northern blot analysis was performed as described (Kishine et al., 2002). The 1.5-kb *Eco*RI fragment of pNNRZ2 was used, which corresponds to the C-terminal half of the NS5A gene and the N-terminal half of the NS5B gene as a probe.

Plasmid construction

pNNRZ2 was used to prepare G418-resistant prototype NN replicon RNA (Kishine et al., 2002). To generate pMH14, L1882L and S2204R mutations in NS4B and NS5A were inserted into pNNRRZ2 by PCR-based site-directed mutagenesis. The following primers were used for mutagenesis: 5′-CTGGTCAATCTACTTCCTGCC-3′ and 5′-GGCAGGAAGTAGATTGACCAG-3′ (Bold letters in the primers denote the substituted nucleotides for L1882L). 5′-CTTCAGCTAGACAGTTGTCTGC-3′ and 5′-GCAGACAACTGTCTAGCTGAAG-3′ (same for S2204R). In addition, 5′-CACCCAAATGTACACC-AATG-3′ and 5′-CGATCCTCATGGAACCGTTC-3′, 5′-GAACGGTTCCATGAGGATCG-3′, and 5′-TGATGGG-CAGCTTGCTTTCC-3′ were used for amplification of appropriate fragments. The *neo* genes in pNNRZ2 and pMH14 were replaced with the luciferase gene from the pGL3 vector (Promega, Tokyo, Japan) to create pLNNRZ2 and pLMH14. To prepare the NS5B (RNA polymerase)-defective luciferase-replicon constructs, we inserted a GHD motif into either pLNNRZ2 or pLMH14 by replacing the corresponding sequence with pNNRZ2GHD (Kishine et al., 2002) to create pLNNRZ2GHD or pLMH14GHD, respectively. pSNC was generated to prepare G418-resistant full-genome replicon cell line, SNC#2. To prepare the plasmid, the sequence from NS3 to the end of the NS5B was cloned from I377NS3-3′ (Lohmann et al., 1999) with the S2204I adaptive mutation and other parts were from pM1LE (Kishine et al., 2002).

The coding region for NS5A in the pNNRZ2 plasmid was cloned into the *Sma*I site of pCALNL5/pBR (kindly provided by Dr. M. Kohara, Tokyo Metropolitan Institute of Medical Science). The neomycin-resistance gene was removed by *Xho*I digestion to prepare the expression vector pcNS5A.

pcDNA3 (Invitrogen)-based plasmids expressing FLAG-tagged human Smad2 or Smad4, HA-tagged constitutively active TGF-β type I receptor (TβR-I[T/D]), and p3TP-Luc have been described previously (Ohshima and Shimotohno, 2003; Imamura et al., 1997). The combined mutant type I receptor, R-ImL45(T/D), which possesses a constitutively active kinase domain, but lacks the ability to phosphorylate Smad, was generated by PCR-based mutagenesis as described (Ohshima and Shimotohno, 2003; Yu et al., 2002). The pAP1-Luc reporter plasmid was obtained commercially (PathDetect Reporter System; Stratagene, LaJolla, CA). Two additional reporter plasmids, pISRE (IFN-α-stimulated response element)-Luc and pGAS (gamma activation site)-Luc, were based on pGL3-Promoter Vector (Promega, Tokyo, Japan) that contains the SV40 basal promoter sequence without an enhancer sequence. To create pISRE-Luc, the ISRE consensus sequence (ACTTT-CAGTTTCAT) was repeated five times in tandem and inserted between the *Mlu*I and *Xho*I cloning sites of the pGL3-Promoter vector. For pGAS-Luc, three tandem repeats of the GAS sequence (TTTCCCCGAAA) were cloned into the pGL3-Promoter Vector at the *Kpn*I–*Bgl*II cleavage site.

RNA synthesis

HCV subgenomic RNA was transcribed in vitro using a MEGAscript T7 kit (Ambion) according to the manufacturer's instructions. Following DNase treatment, RNA was purified by lithium chloride precipitation.

Transfection and luciferase assay

For the luciferase assay to monitor luciferase-replicon, curedMH14 or other cells seeded on 48-well plate (5×10^3 cells/well) were transfected with 0.25 μg of the luciferase-replicon RNA using DMRIE-C reagent (Invitrogen) according to the manufacturer's instructions. Proteins in cells were

extracted in a lysis buffer supplied in a Dual-Luciferase Reporter Assay System (Promega) kit and the luciferase activity was measured using the kit. Assays were performed in triplicate; standard deviations are denoted by bars in the figures. Plasmid DNA was transfected into cells using FuGENE6 reagent (Roche).

Real time RT-PCR analysis

To monitor the effect of cytokines on neo-resistant replicon RNA, TGF-β, IFN-α, or BMP-4 was added in the media of replicon cells seeded on 6-well plate (4 × 10 4 cells/well). At various times, total cellular RNA was collected and subjected to Real time RT-PCR analysis. The 5′-UTR of HCV genomic RNA was quantified using the ABI PRISM 7700 sequence detector (Applied Biosystems) as described (Watashi et al., 2003) using the 5′-CGGGAGAGCCATAGTGG-3′ (forward) and 5′-AGTACCACAAGGCCTTTCG-3′ (reverse) primers and the fluorogenic probe 5′-CTGCGGAACCGGTGAGTACAC-3′. As an internal control, ribosomal RNA was quantified using TaqMan ribosomal RNA control reagents (Applied Biosystems).

Flow cytometry analysis Cells were trypsinized, fixed in formaldehyde, washed with PBS, and treated with staining solution containing 50 μg/ml propidium iodide (PI) (Sigma), 50 μg/ml of RNaseA (Wako), and 0.1% Triton X-100 (nacalai tesque) in PBS for 15 min. PI fluorescence was analyzed using a FACScalibur flow cytometer (Becton Dickinson). Twenty thousand events were collected and analyzed using CellQuest software (Becton Dickinson).

Semi-intact cell replication assay

A semi-intact cell replication assay was performed as described (Miyanari et al., 2003). In brief, cells were permeabilized by incubation in reaction buffer containing digitonin. Following two washes, samples were incubated for 4 h in the labeling reaction mixture containing 10 μCi of [^{32}P]UTP (Amersham Biosciences) in reaction buffer at 27 °C. Total cellular RNA was collected and fractionated by denaturing agarose gel electrophoresis. Radioactivity incorporated into newly synthesized replicon RNA was visualized using a Fujix Bio-Imaging Analyzer BAS2000 System (Fuji Photo Film, Japan).

Metabolic labeling and immunoprecipitation of NS5A protein

Cells were washed in PBS and incubated in methionine-free DMEM (ICN biomedicals) containing 10% dialyzed FBS and 100 μC i/ml of [^{35}S]-methionine (Tran 35S label, ICN biomedicals) for 4 h. After washing in PBS, cells were lysed in RIPA buffer (10 mM Tris-HCl pH 7.4, 1% NP40, 0.1% sodium deoxycholate, 0.1% SDS, 150 mM NaCl, and 1 mM EDTA) for 1 h. Cellular debris was removed by centrifugation at 15,000 rpm for 10 min. Following preclearing, lysates were incubated with a monoclonal antibody against NS5A in the presence of protein-G sepharose. After extensive washing, immune complexes were recovered by low-speed centrifugation and subjected to SDS-PAGE. Radioactivity incorporated into newly synthesized NS5A protein was visualized using a Fujix Bio-Imaging Analyzer BAS2000 System (Fuji Photo Film, Japan).

Acknowledgments

We would like to thank Dr. K. Miyazono for the FLAG-tagged human Smad2, Smad4, TβR-I(T/D) expression plasmids and p3TP-Luc. pCALNL5/pBR and I377/NS3-3′ sequence were kindly provided by Dr. M. Kohara and Dr. R. Bartenschlager, respectively. This work was supported by grants-in-aid for cancer research and by the second-term comprehensive 10-year strategy for cancer control, and by the Ministry of Health, Labor, and Welfare, as well as grants-in-aid for scientific research from the Ministry of Education, Culture, Sports, Science, and Technology, grants-in-aid by the Japanese Society for the Promotion of Science (JSPS), and by the Program for Promotion of Fundamental Studies in Health Science of the Organization for Pharmaceutical Safety and Research (OPSR) of Japan. T. M. is a recipient of a JSPS Postdoctoral Fellowship.

References

Adinolfi, L.E., Utili, R., Andreana, A., Tripodi, M.F., Marracino, M., Gambardella, M., Giordano, M., Ruggiero, G., 2001. Serum HCV RNA levels correlate with histological liver damage and concur with steatosis in progression of chronic hepatitis C. Dig. Dis. Sci. 46 (8), 1677–1683.

Blight, K.J., Kolykhalov, A.A., Rice, C.M., 2000. Efficient initiation of HCV RNA replication in cell culture. Science 290 (5498), 1972–1974.

Calabrese, F., Valente, M., Giacometti, C., Pettenazzo, E., Benvegnu, L., Alberti, A., Gatta, A., Pontisso, P., 2003. Parenchymal transforming growth factor beta-1: its type II receptor and Smad signaling pathway correlate with inflammation and fibrosis in chronic liver disease of viral etiology. J. Gastroenterol. Hepatol. 18 (11), 1302–1308.

Choo, Q.L., Kuo, G., Weiner, A.J., Overby, L.R., Bradley, D.W., Houghton, M., 1989. Isolation of a cDNA clone derived from a blood-borne non-A, non-B viral hepatitis genome. Science 244, 359–362.

Derynck, R., Zhang, Y.E., 2003. Smad-dependent and Smad-independent pathways in TGF-beta family signalling. Nature 425 (6958), 577–584.

Gao, L., Aizaki, H., He, J.W., Lai, M.M., 2004. Interactions between viral nonstructural proteins and host protein hVAP-33 mediate the formation of hepatitis C virus RNA replication complex on lipid raft. J. Virol. 78 (7), 3480–3488.

Gewaltig, J., Mangasser-Stephan, K., Gartung, C., Biesterfeld, S., Gressner, A.M., 2002. Association of polymorphisms of the transforming growth factor-beta1 gene with the rate of progression of HCV-induced liver fibrosis. Clin. Chim. Acta 316 (1–2), 83–94.

Goodman, Z.D., Ishak, K.G., 1995. Histology of hepatitis C virus infection. Semin. Liver Dis. 15, 70–81.

Gressner, A.M., Weiskirchen, R., Breitkopf, K., Dooley, S., 2002. Roles of TGF-beta in hepatic fibrosis. Front. Biosci. 7, 793–807.

Guo, J.T., Sohn, J.A., Zhu, Q., Seeger, C., 2004. Mechanism of the interferon alpha response against hepatitis C virus replicons. Virology 325, 71–81.

Imamura, T., Takase, M., Nishihara, A., Oeda, E., Hanai, J., Kawabata, M., Miyazono, K., 1997. Smad6 inhibits signalling by the TGF-beta superfamily. Nature 389 (6651), 622–626.

Kishine, H., Sugiyama, K., Hijikata, M., Kato, N., Takahashi, H., Noshi, T., Nio, Y., Hosaka, M., Miyanari, Y., Shimotohno, K., 2002. Subgenomic replicon derived from a cell line infected with the hepatitis C virus. Biochem. Biophys. Res. Commun. 293 (3), 993–999.

Liberati, N.T., Datto, M.B., Frederick, J.P., Shen, X., Wong, C., Rougier-Chapman, E.M., Wang, X.F., 1999. Smads bind directly to the Jun family of AP-1 transcription factors. Proc. Natl. Acad. Sci. U.S.A. 96 (9), 4844–4849.

Lohmann, V., Korner, F., Koch, J., Herian, U., Theilmann, L., Bartenschlager, R., 1999. Replication of subgenomic hepatitis C virus RNAs in a hepatoma cell line. Science 285 (5424), 110–113.

Lohmann, V., Hoffmann, S., Herian, U., Penin, F., Bartenschlager, R., 2003. Viral and cellular determinants of hepatitis C virus RNA replication in cell culture. J. Virol. 77 (5), 3007–3019.

Miyanari, Y., Hijikata, M., Yamaji, M., Hosaka, M., Takahashi, H., Shimotohno, K., 2003. Hepatitis C virus non-structural proteins in the probable membranous compartment function in viral genome replication. J. Biol. Chem. 278 (50), 50301–50308.

Miyazono, K., ten Dijke, P., Heldin, C.H., 2000. TGF-beta signaling by Smad proteins. Adv. Immunol. 75, 115–157.

Murphy, F.A., Fauquet, C.M., Bishop, D.H.L., Ghabrial, S.A., Jarvis, A.W., Martelli, G.P., Mayo, M.A., Summers, M.D., 1995. Classification and Nomenclature of Viruses: Sixth Report of the Internal Committee on Taxonomy of Viruses. Springer-Verlag, Viena, Austria, pp. 424–426.

Nelson, D.R., Gonzalez-Peralta, R.P., Qian, K., Xu, Y., Marousis, C.G., Davis, G.L., Lau, J.Y., 1997. Transforming growth factor-beta 1 in chronic hepatitis C. J. Viral Hepatitis 4 (1), 29–35.

Neuman, M.G., Benhamou, J.P., Malkiewicz, I.M., Akremi, R., Shear, N.H., Asselah, T., Ibrahim, A., Boyer, N., Martinot-Peignoux, M., Jacobson-Brown, P., Katz, G.G., Le Breton, V., Le Guludec, G., Suneja, A., Marcellin, P., 2001. Cytokines as predictors for sustained response and as markers for immunomodulation in patients with chronic hepatitis C. Clin. Biochem. 34 (3), 173–182.

Neuman, M.G., Benhamou, J.P., Malkiewicz, I.M., Ibrahim, A., Valla, D.C., Martinot-Peignoux, M., Asselah, T., Bourliere, M., Katz, G.G., Shear, N.H., Marcellin, P., 2002. Kinetics of serum cytokines reflect changes in the severity of chronic hepatitis C presenting minimal fibrosis. J. Viral. Hepat. 9 (2), 134–140.

Ohshima, T., Shimotohno, K., 2003. Transforming growth factor-beta-mediated signaling via the p38 MAP kinase pathway activates Smad-dependent transcription through SUMO-1 modification of Smad4. J. Biol. Chem. 278 (51), 50833–50842.

Scholle, F., Li, K., Bodola, F., Ikeda, M., Luxon, B.A., Lemon, S.M., 2004. Virus-host cell interactions during hepatitis C virus RNA replication: impact of polyprotein expression on the cellular transcriptome and cell cycle association with viral RNA synthesis. J. Virol. 78 (3), 1513–1524.

Shimazaki, T., Honda, M., Kaneko, S., Kobayashi, K., 2002. Inhibition of internal ribosomal entry site-directed translation of HCV by recombinant IFN-alpha correlates with a reduced La protein. Hepatology 35 (1), 199–208.

Shirai, Y., Kawata, S., Tamura, S., Ito, N., Tsushima, H., Takaishi, K., Kiso, S., Matsuzawa, Y., 1994. Plasma transforming growth factor-beta 1 in patients with hepatocellular carcinoma. Comparison with chronic liver diseases. Cancer 73 (9), 2275–2279.

Song, B.C., Chung, Y.H., Kim, J.A., Choi, W.B., Suh, D.D., Pyo, S.L., Shin, J.W., Lee, H.C., Lee, Y.S., Suh, D.J., 2002. Transforming growth factor-beta1 as a useful serologic marker of small hepatocellular carcinoma. Cancer 94 (1), 175–180.

Sumpter Jr., R., Wang, C., Foy, E., Loo, Y.M., Gale Jr., M., 2004. Viral evolution and interferon resistance of hepatitis C virus RNA replication in a cell culture model. J. Virol. 78 (21), 11591–11604.

Taniguchi, H., Kato, N., Otsuka, M., Goto, T., Yoshida, H., Shiratori, Y., Omata, M., 2004. Hepatitis C virus core protein upregulates transforming growth factor-beta 1 transcription. J. Med. Virol. 72 (1), 52–59.

Tanji, Y., Kaneko, T., Satoh, S., Shimotohno, K., 1995. Phosphorylation of hepatitis C virus-encoded nonstructural protein NS5A. J. Virol. 69 (7), 3980–3986.

Ten Dijke, P., Goumans, M.J., Itoh, F., Itoh, S., 2002. Regulation of cell proliferation by Smad proteins. J. Cell. Physiol. 191 (1), 1–16.

Tsushima, H., Kawata, S., Tamura, S., Ito, N., Shirai, Y., Kiso, S., Doi, Y., Yamada, A., Oshikawa, O., Matsuzawa, Y., 1999. Reduced plasma transforming growth factor-beta1 levels in patients with chronic hepatitis C after interferon-alpha therapy: association with regression of hepatic fibrosis. J. Hepatol. 30 (1), 1–7.

Tu, H., Gao, L., Shi, S.T., Taylor, D.R., Yang, T., Mircheff, A.K., Wen, Y., Gorbalenya, A.E., Hwang, S.B., Lai, M.M., 1999. Hepatitis C virus RNA polymerase and NS5A complex with a SNARE-like protein. Virology 263 (1), 30–41.

Wang, C., Pflugheber, J., Sumpter Jr., R., Sodora, D.L., Hui, D., Sen, G.C., Gale Jr., M., 2003. Alpha interferon induces distinct translational control programs to suppress hepatitis C virus RNA replication. J. Virol. 77 (7), 3898–3912.

Watashi, K., Hijikata, M., Hosaka, M., Yamaji, M., Shimotohno, K., 2003. Cyclosporin A suppresses replication of hepatitis C virus genome in cultured hepatocytes. Hepatology 38 (5), 1282–1288.

Yingling, J.M., Datto, M.B., Wong, C., Frederick, J.P., Liberati, N.T., Wang, X.F., 1997. Tumor suppressor Smad4 is a transforming growth factor beta-inducible DNA binding protein. Mol. Cell. Biol. 17 (12), 7019–7028.

Yu, L., Hebert, M.C., Zhang, Y.E., 2002. TGF-beta receptor-activated p38 MAP kinase mediates Smad-independent TGF-beta responses. EMBO J. 21 (14), 3749–3759.

Zhu, H., Liu, C., 2003. Interleukin-1 inhibits hepatitis C virus subgenomic RNA replication by activation of extracellular regulated kinase pathway. J. Virol. 77 (9), 5493–5498.

Original Paper

Intervirology

Intervirology 2005;48:104–111
DOI: 10.1159/000081736

Received: February 5, 2004
Accepted: March 10, 2004

Analysis of the 5′ End Structure of HCV Subgenomic RNA Replicated in a Huh7 Cell Line

Hitoshi Takahashi Masashi Yamaji Masahiro Hosaka Hiroe Kishine
Makoto Hijikata Kunitada Shimotohno

Institute for Virus Research, Kyoto University, Sakyo-ku, Kyoto, Japan

Key Words
Hepatitis C virus · Genome replication · 5′ end · Chronic hepatitis · De novo RNA synthesis

Abstract
Objective: Recently, HCV subgenomic RNA that replicates in vitro in a certain cell line have been elucidated. Since the 5′ end of the genome of positive strand RNA viruses is often modified with a cap structure or a covalently linked protein, we have assessed structural feature of the HCV genome obtained from Huh7 cells in which HCV subgenomic RNA has been shown to efficiently self-replicate. ***Methods:*** HCV subgenomic RNA was obtained from the Huh7 and was analyzed for its 5′ end. ***Results:*** Phosphorylation of the genomic RNA by polynucleotide kinase was observed only after treatment with phosphatase. The labeling efficiency of the genome with polynucleotide kinase was not enhanced by treatment with pyrophosphatase. ***Conclusion:*** It is suggested that the 5′ end of HCV genomic RNA obtained from HCV replicon cells is not modified except phosphorylation. Furthermore, analysis of the 5′ end of the HCV RNA obtained from the HCV subgenome self-replicating cells revealed the presence of two types of subgenomic RNA that contained either guanylate or adenylate at the 5′ end. This result indicates that the 5′ end of the subgenome in Huh7 cells is redundant and there is no significant evolutionary advantage between the two genomes.

Introduction

RNA produced from positive strand RNA viruses in eukaryotes functions as the genome, an intermediate of the genome, and mRNA during viral replication. In these viruses, the 5′ end of the genome is often capped, but there are some exceptions [1]. In the poliovirus, the 5′ end of the genomic RNA is modified by a virally encoded protein, VPg [2]. VPg functions as a primer for poliovirus-encoded RNA polymerase for the synthesis of genomic RNA and the negative strand RNA [3]. Poliovirus mRNA is generated by the cleavage of VPg from the genomic RNA and viral proteins are produced in an internal ribosome entry site (IRES)-dependent manner [4].

The hepatitis C virus (HCV) causes chronic hepatitis C and liver cirrhosis, and has been linked to the develop-

KARGER
Fax + 41 61 306 12 34
E-Mail karger@karger.ch
www.karger.com

0300–5526/05/0483–0104$22.00/0

Accessible online at:
www.karger.com/int

Kunitada Shimotohno
Institute for Virus Research, Kyoto University
Sakyo-ku
Kyoto 606-8507 (Japan)
Tel. +81 75 751 4000, Fax +81 75 751 3998, E-Mail kshimoto@virus.kyoto-u.ac.jp

ment of hepatocellular carcinoma by epidemiological research [5]. HCV is a positive strand RNA virus belonging to the Hepcvirus genus in the *Flaviviridae* family. In this family, there are two additional genera, Flavi- and Pestiviruses. Viral RNA from Flaviviruses has a capped structure and responsive enzymes such as methyltransferase and a capping enzyme are encoded in the viral non-structural (NS) 5 protein, in which RNA polymerase activity also resides [1]. This information suggests that translation of Flavivirus RNA is conducted in a cap-dependent manner. On the other hand, RNA from viruses classified into the Pestivirus and Hepcvirus genera has an IRES structure which plays an important role in cap-independent translation [6, 7].

The HCV genome consists of about 9,600 nucleotides and contains three parts: a 5′ non-coding region of 341 nucleotides containing the sequence for the IRES structure, the coding region of about 3,000 nucleotides, which encodes about 10 viral proteins, and the 3′ non-coding region of about 200 nucleotides depending on the size of the poly-uridylate track within this region [8, 9]. There is no poly-A tail at the 3′ end of the genome; instead, the 3′ end of the genome consists of uridylate [10, 11]. However, the precise structure of the 5′ end of the genome, including possible modifications, remains to be elucidated. Recent progress has established a method that enables the proliferation of the HCV genome in a cell culture system; this also makes it feasible to analyze the biological activity of the HCV genome. Using this system, several HCV sub- and full-genomic RNAs were shown to self-replicate efficiently in certain cell lines, which are known as HCV replicon cells [12]. Although some HCV RNAs synthesized in vitro have proven to be infectious in the chimpanzee, experiments with genomic HCV RNA using this animal model system are laborious [13]. In contrast, HCV replicon cells allow the analysis of the structure of the 5′ end more easily than analysis of samples obtained from liver specimens or sera from HCV-infected individuals. Taking advantage of this opportunity, we have analyzed the 5′ end structure of the HCV genome obtained from HCV replicon cells by assessing the susceptibility to phosphorylation by polynucleotide kinase before and after treatment with enzymes which are used to analyze the 5′ end structure of RNA. Moreover, we have determined the nucleotide residue at the 5′ end of the HCV genomic RNA.

Materials and Methods

Cell Line

MH-14 cells were grown in Dulbecco's modified Eagle medium supplemented with 10% fetal bovine serum, 0.1 m*M* non-essential amino acid mixture and G418.

RNA Extraction

Total RNA from MH-14 cells was extracted by Sepasol I (Nacarai Tesque, Kyoto, Japan) according to the manufacturer's protocol. Extraction of HCV subgenomic RNA was performed with an mRNA isolation kit (Roche, Tokyo) using a biotin-labeled oligonucleotide probe, 5′-biotin-TAGGATTCGTGCTCATGGTTGCACGGTCTACGAGAC-3′, which is complementary to the 5′ non-coding region of the HCV genome. The bound HCV RNA was trapped in an avidin-linked resin through the oligonucleotide and eluted from the resin by heat.

Modification of RNA by Various Enzymes

RNA was treated with 0.2 unit of bacterial alkaline phosphatase, BAP, in 0.1 *M* Tris-HCl (pH 8.0), 1 m*M* $MgSO_4$, and 40 units of RNase inhibitor (Applied Biosystems) and then subjected to a polynucleotide kinase reaction in the presence of ^{32}P-γ-ATP in 10 m*M* Tris-acetate (pH 7.6), 10 m*M* MgOAc, 50 m*M* potassium acetate, 0.185 Mbq ^{32}P-γ-ATP, and 40 units of RNase inhibitor at 37°C for 30 min. For the treatment by pyrophosphatase, RNA was incubated with 5 units of tobacco acid pyrophosphatase (TAP) in a buffer consisting of 50 m*M* sodium acetate (pH 5.0), 0.1% β-mercaptoethanol, 1 m*M* EDTA, 0.01% Triton X-100 and 40 units of RNase inhibitor at 37°C for 30 min. Following TAP treatment, the RNA was further treated with BAP and subjected to polynucleotide kinase reaction. The in vitro synthesized HCV subgenomic RNA was treated with BAP and polynucleotide kinase as described above.

Analysis of Mononucleotides by Thin-Layer Chromatography

The 5′ end labeled RNA was extracted from the agarose gel and was treated with 0.3 *N* NaOH for 24 h at 37°C to hydrolyze the RNA to mononucleotides. The digest was desalted by DEAE Sepharose column chromatography and subjected to thin-layer chromatography. The thin-layer plate was developed with the solvents consisting of isobutylic acid and 0.5 *M* ammonia water (5:3, vol/vol) in the first dimension, and with a solvent consisting of isopropanol, 12 *N* HCl and H_2O in volume ratios of 70:15:15 for the 2nd dimension. The signal was detected by autoradiography. The identity of each spot was determined by co-development of authentic mononucleotides in the chromatography.

Analysis of the 5′ End of RNA by Rapid Amplification of cDNA ENDs, RACE

RNA was treated with BAP and subjected to a polynucleotide kinase reaction. After this treatment, a 5′-CCCGUCUUCGGACAUCCAGAGGUAC-3′ RNA oligomer was ligated to the RNA. Reverse transcription followed by PCR was conducted using the following primers: 5′-CGCGGATCCCCCGTCTTCGGACATCCA-3′, which contains part of the sequence of the RNA oligomer, and 5′-CCGGAATTCACGCTTTCTGCGTGAAGACAG-3′, which is complementary to the 5′ region of the HCV genome. The RACE experiment was conducted according to the manufacturer's protocol. The amplified DNA was cloned into a TA-plasmid and sequenced.

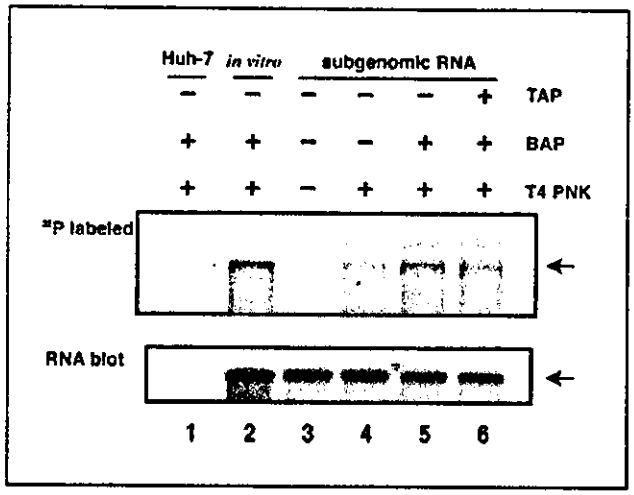

Fig. 1. Analysis of the 5′ end of HCV subgenomic RNA isolated from the HCV genome self-replicating cell line, Huh7. MH14 cells (10^7 cells), which allow the self-replication of the HCV subgenome, were harvested and total RNA was prepared using Sepasol I. The total RNA was then incubated with a biotinylated oligoDNA fragment which is complementary to the non-coding region of the HCV genome as described in Materials and Methods. The RNA was divided into three aliquots. The first RNA aliquot was treated with BAP followed by labeling of its end with a polynucleotide kinase reaction in the presence of ^{32}P-γ-ATP. The second RNA aliquot was treated with 5 units of TAP, BAP and followed by end-labeling. The third RNA aliquot was pretreated in a similar way, but without addition of any enzymes, and subjected to polynucleotide kinase reaction. The in vitro synthesized HCV subgenomic RNA was treated with BAP and polynucleotide kinase as described. Each aliquot of RNA was then divided in half and the RNAs were electrophoresed on two denaturing agarose gels in MOPS buffer. One gel was dried and analyzed by autoradiography and the other gel was subjected to Northern blot using a radio-labeled HCV RNA probe.

Results and Discussion

Analysis of the 5′ End Structure of HCV Subgenomic RNA Isolated from an HCV Replicon Cell Line, MH-14

We have previously established HCV replicon cells derived from the Huh7 cell line by transfecting HCV genomic RNA synthesized in vitro. The RNA was synthesized using information about infectious HCV RNA obtained from a human T lymphocytes line, MT-2, infected with HCV-positive plasma [14]. There were approximately a few thousand copies of HCV subgenomic RNA per replicon cell as determined by real-time reverse transcription followed by polymerase chain reaction (RT-PCR) [15, 16]. During proliferation of the HCV replicon cells, we obtained one cell clone, MH14, in which the level of HCV subgenomic RNA was 3- to 4-fold higher than in the original replicon cells [17]. The increased copy number seemed to be the result of the evolution of the HCV subgenomic RNA by nucleotide substitution as has been previously described by other groups [18]. A detailed analysis of the genome in the cell clone was reported elsewhere [19].

Total RNA from MH-14 cells was extracted by the method described in Materials and Methods. Using this method, only positive strand genomic RNA was extracted (fig. 1, data not shown). The extracted HCV RNA was divided into three aliquots. One aliquot was used without further enzymatic modification, the second aliquot was treated with bacterial alkaline phosphatase (BAP) alone, and the third aliquot was treated with tobacco acid pyrophosphatase (TAP) (Epicenter, Wisc., USA), followed by treatment with BAP. A polynucleotide kinase reaction was then carried out on all three aliquots. To generate control HCV RNA, the plasmid pNNRZ2, which carries the entire subgenome of the HCV replicon used to establish the HCV replicon cell line, was in vitro transcribed by T7 RNA polymerase. The RNA was purified by DNase I treatment followed by phenol-chloroform treatment. HCV subgenomic RNA from each preparation was semiquantitated by RT-PCR and equal amounts of HCV subgenomic RNA were radio-labeled by polynucleotide kinase reaction using ^{32}P-γ-ATP. As a control, the in vitro synthesized HCV subgenomic RNA was subjected to the polynucleotide kinase reaction in the presence of ^{32}P-γ-ATP before and after treatment with BAP. Following the polynucleotide kinase reaction, the RNA was electrophoresed in a denaturing agarose gel and subjected to autoradiography. A signal at 8 kb, the position of the intact subgenomic RNA, is expected if ^{32}P is incorporated at the 5′ end of the HCV subgenomic RNA. A very faint autoradiographic signal was detectable from the in vitro synthesized RNA subjected to the kinase reaction without BAP treatment (data not shown). In contrast, a significant incorporation of ^{32}P was observed in the sample treated with BAP prior to the polynucleotide kinase reaction (fig. 1). This result indicates that the in vitro synthesized HCV subgenomic RNA was phosphorylated at the 5′ terminus and, as expected, was resistant to the kinase reaction. Next, we conducted a kinase reaction on the HCV subgenomic RNA prepared from MH-14 cells. When the HCV RNA was subjected to the kinase reaction without BAP treatment, only a slight ^{32}P signal was detected. The level of ^{32}P incorporation increased when the kinase reaction was carried out after treatment with BAP (fig. 1,

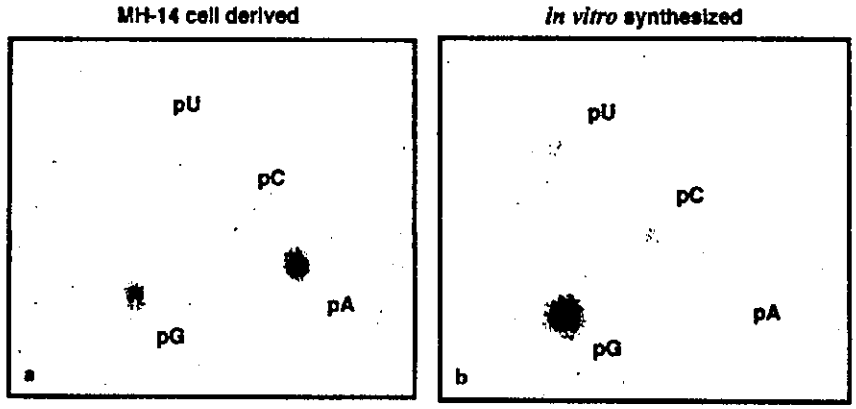

Fig. 2a, b. Analysis of nucleoside monophosphate derived from the 5′ end of the HCV subgenomic RNA. 5′ end labeled RNA as shown in figure 1, lanes 2 and 5, was extracted from the agarose gel. This RNA was treated with 0.3 *N* NaOH for 24 h at 37°C to hydrolyze the RNA to mononucleotides. The digest was desalted by DEAE Sepharose column chromatography and subjected to thin-layer chromatography. The thin-layer plate was developed with the solvents described in the text, and the signal was detected by autoradiography. The identity of each spot was determined by co-development of authentic mononucleotide in the chromatography.

lanes 4 and 5). When HCV subgenomic RNA was treated with TAP, BAP, and then subjected to the kinase reaction, the amount of incorporation of ^{32}P was very similar to that of incorporation observed without TAP treatment (fig. 1, lanes 5 and 6). An RNA fraction obtained from Huh7 cells by the same procedure used to prepare the HCV subgenomic RNA from HCV replicon cells was used as a negative control. This RNA did not give rise to any ^{32}P signal after the kinase reaction either before or after BAP treatment (fig. 1, lane 1). To confirm that the differences in the intensity of the bands detected by autoradiography were not dependent on the amount of HCV RNA used for the analysis, the amount of RNA was analyzed by northern blot and was confirmed to be in almost the same range (fig. 1, lower panel). It is worth mentioning that the intensity of the ^{32}P signal detected in in vitro synthesized HCV RNA and the RNA obtained from Huh7 cells was almost the same (fig. 1, lanes 2 and 5). Taken together, these results indicate that the 5′ end of the majority of the HCV subgenomic RNA replicating in Huh7 cells was sensitive to BAP treatment. The fact that the phosphate residues at the end of the HCV genomic RNA were labile to BAP, and that TAP plus BAP treatment did not enhance the incorporation of ^{32}P, suggests that the 5′ end of the HCV genome does not contain a modification such as a cap or a protein linked covalently through the 5′ phosphate residue. However, the following possibilities exist: the presence of a modified structure which is resistant to pyrophosphatase treatment or the presence of a modification that does not interfere with the 5′ phosphate residue.

Whereas the poliovirus genomic RNA contains VPg, the poliovirus mRNA lacks VPg at its 5′ end, despite the fact that the nucleotide sequence of the end is the same in both genomic and messenger RNAs [20]. Considering the characteristics of poliovirus RNA polymerase, it is likely that the VPg at the end of the genomic RNA is cleaved off to generate functional mRNA. By analogy to poliovirus replication, it remains a possibility that the abundant HCV RNA in HCV replicon cells is an unmodified mRNA type, but not a genomic type. However, as described below, we think this possibility is unlikely.

Poliovirus RNA polymerase can synthesize RNA complementary to the template only in the presence of a primer RNA or in the presence of VPg in vitro [4]. However, under physiological conditions, the polymerase uses VPg as the primer exclusively. Poliovirus polymerase incorporates uridylate at the tyrosine residue of VPg and an RNA elongation reaction proceeds via addition of a nucleotide complementary to the template at the 3′ end of the uridylate residue. On the other hand, HCV NS5B does not depend on the presence of a primer for the initiation of RNA synthesis in vitro. Differences in this characteristic feature of these two enzymes also support the possibility that the HCV genome does not have a 5′ modified structure such as that of poliovirus genomic RNA.

Analysis of the Nucleotide at the 5′-Terminus of the HCV Subgenomic RNA Replicated in HCV Replicon Cells

To further analyze the structure of the 5′ end of the HCV subgenomic RNA present in the HCV replicon Huh7 cells, we radiolabeled the 5′ end with polynucleotide kinase after BAP treatment and the RNA was electrophoresed in a denaturing agarose gel as shown in figure 1. The 8-kb RNA was eluted from the gel and treated with 0.3 *N* NaOH for 24 h at 37°C. The resulting nucleotide solution was subjected to two-dimensional thin-layer

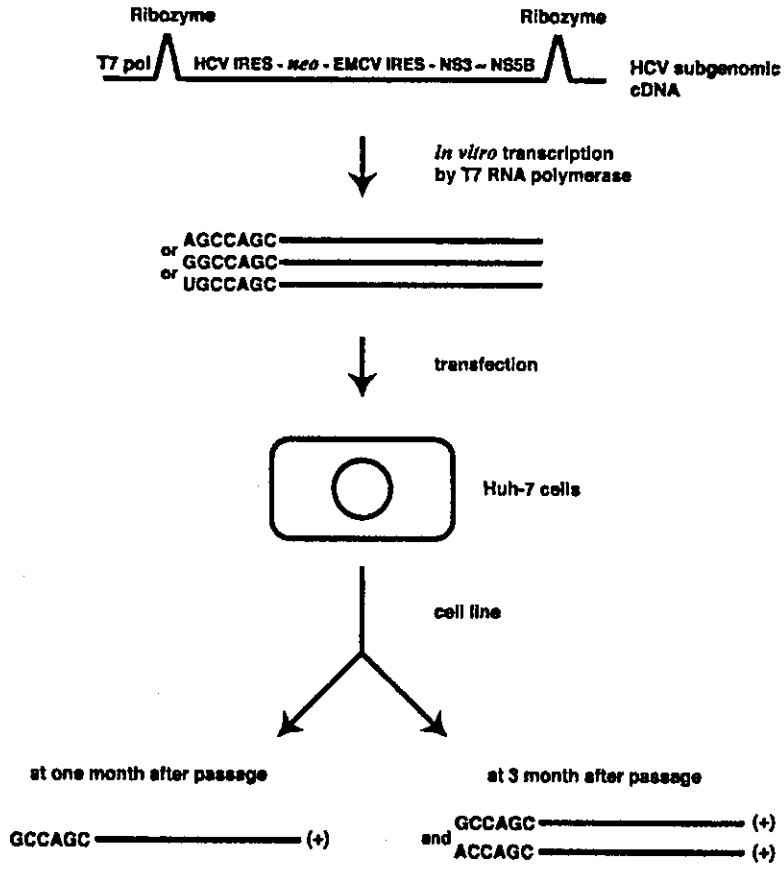

Fig. 3. A brief diagram of the HCV subgenomic RNA used to establish HCV genome replicon cells, the experimental procedure for analysis of the 5′-terminal structure, and the results of the nucleotide sequence of the 5′ end of the genome.

chromatography and developed with a solvent described in Materials and Methods. The thin layer plate was exposed to an X-ray film after development (fig. 2a). The HCV subgenomic RNA synthesized in vitro was analyzed in the same way (fig. 2b). The RNA synthesized in vitro is expected to have guanylate at the 5′ end, as determined by the structure of the pNNRZ2 plasmid. Indeed, the observed result agreed with the expectation. In addition to the major guanylate (GMP) spot, spots corresponding to uridylate (UMP), cytidylate (CMP) and adenylate (AMP) were faintly detectable. We think that the ^{32}P-UMP, ^{32}P-CMP and ^{32}P-AMP were generated by a kinase reaction acting on partially degraded HCV genomic RNA. In contrast, the RNA from the HCV replicon Huh7 cell line, MH14, gave rise to production of ^{32}P-GMP and ^{32}P-AMP as major spots, in addition to production of small amounts of ^{32}P-UMP and ^{32}P-CMP. The UMP and CMP are likely derived from RNA contaminants in the preparation of HCV genomic RNA. The same result was observed in an analysis of the 5′ end of the HCV genome prepared from other HCV replicon cells (data not shown). Sequence data shows that the first adenylate residue downstream of the 5′ end of the genome is located at 4th base into the sequence. Thus, it is unlikely that this adenylate residue correlates to the end of the HCV subgenome in HCV replicon cells. Rather, it seems more likely that the 5′ terminal nucleotide has been converted to adenylate from guanylate during genomic replication in the replicon cells. To confirm this possibility we conducted RACE to analyze the 5′ end structure of the HCV subgenomic RNA.

First, we analyzed the 5′ end structure of the HCV subgenome in HCV replicon cells that were established by introduction of three independent HCV subgenomes with different bases at the 5′ end. We synthesized three types of HCV subgenomes by in vitro transcription; one type had an extra adenylate at the 5′ end, the second had an extra

uridylate at the 5′ end, and the third had an extra guanylate at the 5′ end. Other than this initial extra residue, the three types of subgenome had the same nucleotide sequences. After transfection of each RNA into Huh7 cells, transfected cells were selected by adding G418 to the culture medium. The clones obtained from cells transfected with each genomic RNA were pooled and expanded to about 5 million cells and the 5′ end of the HCV subgenome in each group was analyzed by RACE as described in 'Materials and Methods'. The data demonstrated that the nucleotide at each of the 5′ end of the HCV genomes was exclusively guanlyate in all HCV replicon cell lines when analyzed them at the early stage, most likely in a month, of the establishment of cell lines (fig. 3; data not shown). This is consistent with data reported previously by another group using an animal model [13]. Next, we analyzed the HCV subgenomic RNA in the HCV replicon cell lines at about 3 months after they were established. Surprisingly, the 5′ end structure of the HCV genomic RNA obtained from the cells was 5′GCC--- in 11 clones and 5′ACC--- in 18 clones.

Finding adenylate at the 5′ end of the genome suggests the possibility of some intriguing mechanism for the initiation of RNA synthesis by NS5B in HCV replicon cells. The initiation of the genome might start not only with guanylate but also with adenylate. It is also possible that the synthesis of the negative strand RNA of the HCV subgenome, in particular the incorporation of the 3′ end nucleotide, may be redundant: G:C pairing and G:U pairing may occur, interactions of which are often shown in RNA molecules such as tRNA.

NS5B has been shown to synthesize RNA in a template-dependent manner via a primer-independent (de novo) mechanism in vitro [21, 22]. During polymerization by NS5B in vitro, the kinetics of the initiation of RNA synthesis depend on the concentration of substrates, and the 3′ end sequence of the template. NS5B preferred ATP and GTP as the first initiator nucleotide for de novo RNA synthesis when the 3′ end of the HCV genome, the sequence of which is ---GU_{OH} 3′, was used as a template [21, 22]. Selection of guanylate by NS5B as an initiator nucleotide may be achieved by the formation of a basepair of guanylate with the terminal uridylate. Moreover, using various templates with different nucleotide sequences, the selection efficiency of the nucleotide at the initiation of RNA synthesis is in the order GTP>ATP≫CTP⋙UTP [23]. If the nucleotide at the 3′ end of a template is a less preferred nucleotide for NS5B in de novo synthesis of RNA, the penultimate base, if preferred by the enzyme, is used as the initiator base for synthesis of RNA. However, the fidelity of NS5B in choosing the initiation nucleotide is still unclear. Moreover, the biochemical analysis of the polymerase activity of NS5B in vitro was conducted in the presence of NS5B alone. Recent reports have demonstrated that NS5B associates with NS5A, another HCV nonstructural protein [24]. Thus, it is possible that characteristics of the enzymatic activity of NS5B may be modified by such an interaction in vivo.

^{32}P-AMP and -GMP spots detected by thin-layer chromatography co-migrated and overlapped well with authentic AMP and GMP markers (fig. 2). This evidence indicates that there is no modification on either of these nucleotides, and also strongly supports the idea that the 5′ end of the HCV genome is phosphorylated but remains free from other modifications.

Determination of the crystallographic structures of the active site domains of many RNA-dependent RNA polymerases (RdRp) has revealed an evolutionary link between HCV NS5B and the catalytic subunit of bacteriophage Φ6 RdRp, which also initiates RNA synthesis in a de novo manner [25]. According to the model of the initiation of RNA synthesis by Φ6 RNA polymerase, a base at the penultimate position at the 3′ end of the template pairs with the complementary nucleoside triphosphate. Next, a substrate basepair forms at the 3′ end base which aligns the specific binding pocket (site S) according to Butcher et al. [25]. After formation of the basepairs, these two nucleotides are covalently linked by a phosphodiester bond and the elongation process occurs. Although the authors suggested that this mechanism is applicable to the initiation reaction for de novo RNA synthesis by HCV NS5B, this conclusion is debatable [26]. Thus, more work is required to clarify the precise molecular mechanism of de novo RNA synthesis by NS5B.

As mentioned above, efficient incorporation of ^{32}P-γ-GMP into the RNA synthesized de novo by NS5B in an in vitro reaction was observed when the 3′ end of the HCV genome was used as a template. This is likely due to the formation of a basepair between guanosine triphosphate and uridylate, the base at the 3′ end of the template. It is unclear whether the formation of a G:U pair occurs between the 5′ end of the HCV genome and the 3′ end of its complementary strand in vivo. However, if such a basepair forms with some frequency, the structure of the 3′ end of the complementary strand of the genome would be changed from 3′CGG---5′ to a sequence of 3′UGG---5′. In this case, de novo synthesis of the HCV genomic RNA would start with A rather than G. Thus, detection of AMP at the 5′ end of the HCV subgenome may be explained by redundant basepairing at the 5′ end.

Nucleotide sequences of the HCV genome derived from various sources have been reported [27]. The nucleotide at the 5′ end of the HCV genome was reported to be either adenylate or guanylate, although uridylate or guanylate were also present at the end in a few cases. Adenylate residue at the 5′ end is preferred in some HCV genotypes, such as HCV-3a and HCV-2a, and a 5′ guanylate residue is preferred in other HCV genotypes, including HCV-1a and -1b. These data are significantly different from our observation that HCV genomes with guanylate or adenylate at the 5′ end are almost equally represented in Huh7 replicon cells which were established by introducing HCV subgenomic RNA of the 1b type. Although we do not know the reason for the presence of two types of HCV genome in these cells, there are at least two possibilities: (1) evolutional selection between HCV genomes with differing 5′ residues in the HCV replicon cells is negligible, and (2) the mechanism of initiation of HCV RNA synthesis in the HCV replicon cells is somehow different from the initiation of RNA synthesis in hepatocytes in vivo.

Phylogenetic analyses of the HCV genome has shown that the evolutionary distance between HCV-3a and HCV-2a is greater than the distance between HCV-3a and HCV-1b [27]. However, HCV-3a and HCV-2a have a genome containing predominantly adenylate at the 5′ end while the HCV-1b genome contains guanylate at its 5′ end. Importantly, HCV genomes incorporating guanylate or adenylate at the 5′ end are sporadically present in HCV-3a or HCV-1b, respectively. This observation, together with our findings, suggests that HCV NS5B might have had a similar ability to initiate de novo RNA synthesis with adenylate or guanylate during the early stages of its evolution. NS5B may then have gradually acquired a mechanism to select a specific initiator nucleotide in certain HCV genotypes. However, this selective mechanism may be lost when the HCV genome is replicated under in vitro conditions, such as in Huh7 cells. Clarification of the precise molecular mechanism of de novo RNA synthesis by NS5B may help to clarify this possibility.

Acknowledgements

The authors acknowledge to the member of the Department of Viral Oncology for their helps and suggestion to this work. This work was supported by Grants-in-Aid for cancer research and for the Second-term Comprehensive 10-year Strategy for Cancer Control from the Ministry of Health, Labor, and Welfare, through grants-in-aid for scientific research from the Ministry of Education, Culture, Sports, Science and Technology, Grants-in-Aid for research for the future from the Japanese Society for the Promotion of Science, and by the Program for Promotion of Fundamental Studies in Health Science of the Organization for Pharmaceutical Safety and Research (OPSR) of Japan.

References

▶1 Egloff MP, Benarroch D, Selisko B, Romette JL, Canard B: An RNA cap (nucleoside-2′-O-)-methyltransferase in the flavivirus RNA polymerase NS5:crystal structure and functional characterization. EMBO J 2002;21:2757–2768.

2 Lee YF, Nomoto A, Detjen BM, Wimmer E: A protein covalently linked to poliovirus genome RNA Proc Natl Acad Sci USA 1977;74:59–63.

3 Nomoto A, Detjen B, Pozzatti R, Wimmer E: The location of the polio genome protein in viral RNAs and its implication for RNA synthesis. Nature 1977;268:208–213.

▶4 Paul AV, van Boom JH, Filippov D, Wimmer E: Protein-primed RNA synthesis by purified poliovirus RNA polymerase. Nature 1998;393: 280–284.

▶5 Shimotohno K: Hepatitis C virus as a causative agent of hepatocellular carcinoma. Intervirology 1995;38:162–169.

▶6 Tsukiyama-Kohara K, Iizuka N, Kohara M, Nomoto A: Internal ribosome entry site within hepatitis C virus RNA. J Virol 1992;66:1476–1483.

▶7 Wang C, Sarnow P, Siddiqui A: Translation of human hepatitis C virus RNA in cultured cells is mediated by an internal ribosome-binding mechanism. J Virol 1993;67:3338–3344.

▶8 Choo QL, Richman KH, Han JH, Berger K, Lee C, Dong C, Gallegos C, Coit D, Medina-Selby R, Barr PJ, et al: Genetic organization and diversity of the hepatitis C virus. Proc Natl Acad Sci USA 1991;88:2451–2455.

▶9 Kato N, Hijikata M, Ootsuyama Y, Nakagawa M, Ohkoshi S, Sugimura T, Shimotohno K: Molecular cloning of the human hepatitis C virus genome from Japanese patients with non-A, non-B hepatitis. Proc Natl Acad Sci USA 1990;87:9524–9528.

▶10 Tanaka T, Kato N, Cho MJ, Shimotohno K: A novel sequence found at the 3′ terminus of hepatitis C virus genome. Biochem Biophys Res Commun 1995;215:744–749.

▶11 Tanaka T, Kato N, Cho MJ, Sugiyama K, Shimotohno K: Structure of the 3′ terminus of the hepatitis C virus genome. J Virol 1996;70: 3307–3312.

▶12 Lohmann V, Korner F, Koch J, Herian U, Theilmann L, Bartenschlager R: Replication of subgenomic hepatitis C virus RNAs in a hepatoma cell line. Science 1999;285:110–113.

▶13 Kolykhalov AA, Agapov EV, Blight KJ, Mihalik K, Feinstone SM, Rice CM: Transmission of hepatitis C by intrahepatic inoculation with transcribed RNA. Science 1997;277:570–574.

▶14 Sugiyama K, Kato N, Mizutani T, Ikeda M, Tanaka T, Shimotohno K: Genetic analysis of the hepatitis C virus (HCV) genome from HCV-infected human T cells. J Gen Virol 1997;78(Pt 2):329–336.

15 Takeuchi T, Katsume A, Tanaka T, Abe A, Inoue K, Tsukiyama-Kohara K, Kawaguchi R, Tanaka S, Kohara M: Real-time detection system for quantification of hepatitis C virus genome. Gastroenterology 1999;116:636–642.

▶16 Kishine H, Sugiyama K, Hijikata M, Kato N, Takahashi H, Noshi T, Nio Y, Hosaka M, Miyanari Y, Shimotohno K: Subgenomic replicon derived from a cell line infected with the hepatitis C virus. Biochem Biophys Res Commun 2002;293:993–999.

17 Miyanari Y, Hijikata M, Yamaji M, Hosaka M, Takahashi H, Shimotohno K: Hepatitis C virus Non-structural proteins in the probable membranous compartment function in viral RNA replication. J Biol Chem 2003;278: 50301–50308.
▶18 Lohmann V, Korner F, Dobierzewska A, Bartenschlager R: Mutations in hepatitis C virus RNAs conferring cell culture adaptation. J Virol 2001;75:1437–1449.
▶19 Krieger N, Lohmann V, Bartenschlager R: Enhancement of hepatitis C virus RNA replication by cell culture-adaptive mutations. J Virol 2001;75:4614–4624.
20 Nomoto A, Kitamura N, Golini F, Wimmer E: The 5'-terminal structures of poliovirion RNA and poliovirus mRNA differ only in the genome-linked protein VPg. Proc Natl Acad Sci USA 1977;74:5345–5349.
▶21 Zhong W, Uss AS, Ferrari E, Lau JY, Hong Z: De novo initiation of RNA synthesis by hepatitis C virus nonstructural protein 5B polymerase. J Virol 2000;74:2017–2022.
▶22 Kim M, Kim H, Cho SP, Min MK: Template requirements for de novo RNA synthesis by hepatitis C virus nonstructural protein 5B polymerase on the viral X RNA. J Virol 2002;76: 6944–6956.
▶23 Lohmann V, Roos A, Korner F, Koch JO, Bartenschlager R: Biochemical and structural analysis of the NS5B RNA-dependent RNA polymerase of the hepatitis C virus. J Viral Hepatol 2000;7:167–174.
▶24 Shirota Y, Luo H, Qin W, Kaneko S, Yamashita T, Kobayashi K, Murakami S: Hepatitis C virus (HCV) NS5A binds RNA-dependent RNA polymerase (RdRP) NS5B and modulates RNA-dependent RNA polymerase activity. J Biol Chem 2002;277:11149–11155.
▶25 Butcher SJ, Grimes JM, Makeyev EV, Bamford DH, Stuart DI: A mechanism for initiating RNA-dependent RNA polymerization. Nature 2001;410:235–240.
▶26 O'Farrell D, Trowbridge R, Rowlands D, Jager J: Substrate complexes of hepatitis C virus RNA polymerase (HC-J4): Structural evidence for nucleotide import and de-novo initiation. J Mol Biol 2003;326:1025–1035.
27 HCV database: http://s2as02.genes.nig.ac.jp/index.html

THE JOURNAL OF BIOLOGICAL CHEMISTRY
© 2005 by The American Society for Biochemistry and Molecular Biology, Inc.

Vol. 280, No. 18, Issue of May 6, pp. 18355–18360, 2005
Printed in U.S.A.

Role of Cyclophilin B in Activation of Interferon Regulatory Factor-3*

Received for publication, February 14, 2005
Published, JBC Papers in Press, March 10, 2005, DOI 10.1074/jbc.M501684200

Yoko Obata‡, Kazuo Yamamoto‡, Masanobu Miyazaki‡, Kunitada Shimotohno§, Shigeru Kohno‡, and Toshifumi Matsuyama‡¶

From the ‡Department of Molecular Microbiology and Immunology, Nagasaki University Graduate School of Biomedical Sciences, 1-12-4 Sakamoto, Nagasaki 852-8523 and the §Department of Viral Oncology, Institute for Virus Research, Kyoto University, Sakyo-ku, Kyoto 606-8507, Japan

IRF-3 is a member of the interferon regulatory factors (IRFs) and plays a principal role in the induction of interferon-β (IFN-β) by virus infection. Virus infection results in the phosphorylation of IRF-3 by IκB kinase ε and TANK-binding kinase 1, leading to its dimerization and association with the coactivators CREB-binding protein/p300. The IRF-3 holocomplex translocates to the nucleus, where it induces IFN-β. In the present study, we examined the molecular mechanism of IRF-3 activation. Using bacterial two-hybrid screening, we isolated molecules that interact with IRF-3. One of these was cyclophilin B, a member of the immunophilins with a *cis-trans* peptidyl-prolyl isomerase activity. A GST pull-down assay suggested that one of the autoinhibition domains of IRF-3 and the peptidyl-prolyl isomerase domain of cyclophilin B are required for the binding. A knockdown of cyclophilin B expression by RNA interference resulted in the suppression of virus-induced IRF-3 phosphorylation, leading to the inhibition of the subsequent dimerization, association with CREB-binding protein, binding to the target DNA element, and induction of IFN-β. These findings indicate that cyclophilin B plays a critical role in IRF-3 activation.

Interferon regulatory factors (IRF(s))[1] are a family of transcription factors that regulate a variety of biological events, including innate immunity. Once activated by the invasion of a pathogen, such as viruses and bacteria, IRFs regulate the expression of various genes encoding immunomodulatory cytokines and chemokines and limit the spread of infection. Among these factors, interferons (IFNs) play important roles in host defense, cell growth regulation, and immune activation (1, 2). IFNs include the type I IFN-αs and IFN-β and the type II IFN-γ. Type I IFNs are immediately induced in response to various viral infections, and IRF-3 and IRF-7 play an important role in their induction (3, 4). The mode of IRF-3 involvement against virus infection has been analyzed by using Newcastle disease virus (NDV) and Sendai virus (5–9). IRF-3 is expressed in the cytoplasm as a latent, inactive form, and its C-terminal serine/threonine residues are phosphorylated by IκB kinase ε and TANK-binding kinase 1 (10, 11). Virus-induced C-terminal phosphorylation of IRF-3 represents an important posttranslational modification, leading to dimerization (6, 7), translocation from the cytoplasm to the nucleus, association with CBP/p300 coactivators (6, 9), stimulation of DNA binding to the IFN-stimulated response elements (ISREs), and activation of the corresponding genes (5, 8, 9).

IRF-3 consists of an N-terminal DNA-binding domain that specifically binds to an ISRE motif, and a C-terminal IRF association domain (IAD) that mediates protein-protein interactions. IRF-3 uses the IAD for both intramolecular autoinhibition interactions and intermolecular dimerizations (6, 12). Furthermore, IRF-3 possesses a transactivation domain (amino acids 134–394) and two autoinhibition domains found within the proline-rich sequence (amino acids 134–197) and at the C-terminal end (amino acids 407–414). The two autoinhibition domains are thought to interact with each other to generate a closed conformation that masks the C-terminal IAD, the DNA-binding domain, and the nuclear localization signal of IRF-3, which prevents homodimerization and DNA binding in uninfected cells. The C-terminal phosphorylation of IRF-3 might open the conformation, leading to dimer formation and exposure of the nuclear localization signal and the DNA-binding domain (6, 13, 14). However, the molecular events associated with such a drastic conformational change remain unknown. In the present study, we demonstrate the interaction of IRF-3 with cyclophilin B (CypB), an immunophilin with *cis-trans* peptidyl-prolyl isomerase and chaperone-like activities (15). The knockdown of CypB by RNA interference prevented the NDV-induced IRF-3 phosphorylation, dimerization, association with CBP, binding to the ISRE, and induction of IFN-β.

EXPERIMENTAL PROCEDURES

Bacterial Two-hybrid Screening—A BacterioMatch™ two-hybrid SystemXR Plasmid cDNA library (Stratagene, La Jolla, CA) was used to screen IRF-3 interacting proteins according to the manufacturer's protocol. For the construction of the bait plasmid, the GST fusion expression plasmid pGEX-IRF-3 was digested at the NcoI site, which overlapped with the initiation codon of IRF-3, filled in with the Klenow fragment of DNA polymerase I, and then digested by XhoI. The plasmid pBT was digested by BamHI, filled in with the Klenow fragment of DNA polymerase I, and then digested by XhoI. The NcoI/Klenow-XhoI fragment containing the IRF-3 coding region was ligated with the pBT fragment. The junction of the cloning site of the resultant plasmid pBT-IRF-3 was verified by sequencing. Competent cells of the BacterioMatch two-hybrid system *Escherichia coli* reporter strain were transformed with pBT-IRF-3, together with the pTRG-cDNA library (Human HeLa cell plasmid cDNA library, number 982208, Stratagene). As every

* This work was supported by a grant-in-aid from the Ministry of Education, Culture, Sports, Science, and Technology and by the 21st Century Center of Excellence Program of Nagasaki University. The costs of publication of this article were defrayed in part by the payment of page charges. This article must therefore be hereby marked "*advertisement*" in accordance with 18 U.S.C. Section 1734 solely to indicate this fact.

¶ To whom correspondence should be addressed. Tel.: 81-95-849-7081; Fax: 81-95-849-7083; E-mail: tosim@net.nagasaki-u.ac.jp.

[1] The abbreviations used are: IRF, interferon regulatory factor; IFN, interferon; CBP, cAMP-response element-binding protein-binding protein; ISRE, interferon-stimulated response element; NDV, Newcastle disease virus; ISG, interferon-stimulated gene; GST, glutathione *S*-transferase; CypB, cyclophilin B; PPIase, peptidyl-prolyl isomerase; siRNA, small interfering RNA.

transformation produced 4.0–5.0 × 10^5 clones, we finally screened 4.30 × 10^6 colonies after 10 transformations. The cDNA-containing plasmids were recovered from the antibiotic-resistant and *lacZ*-positive clones, and the sequences of the cDNA inserts were verified, using the pTRG forward primer (5′-CAGCCTGAAGTGAAAGAA-3′) and the pTRG reverse primer (5′-ATTCGTCGCCCGCCATAA-3′), by a PRISM 310 or 3100 autosequencer. For the construction of the N-terminal Myc-tag fusion protein expression vector, a synthetic oligonucleotide containing the Myc-tag sequence, followed by HindIII, NcoI, BamHI, NotI, and EcoRI sites as multicloning sites, was ligated into pcDNA3 digested with HindIII and EcoRI to yield the plasmid pcDNA/Myc. The cDNAs of the candidate positive clones were amplified by PCR with the pTRG forward and reverse primers, digested with BamHI, NotI, or EcoRI for the 5′-junction and XhoI for the 3′-junction, and then subcloned into the corresponding sites of pcDNA3/Myc.

GST Pull-down Assay—The Myc-tagged protein encoded by the cloned cDNA was synthesized by the TnT Quick Coupled Transcription/Translation Systems (Promega) with unlabeled methionine. To construct the plasmids pGEX-hIRF-3ΔN1–3, pGEX-hIRF-3 was digested with ScaI, MscI, or BglII, blunt-ended with the Klenow enzyme, and then digested with SacII. The 938-bp ScaI-SacII fragment, the 608-bp MscI-SacII fragment, and the 350-bp BglII-SacII fragment were excised and subcloned into the blunt-ended NcoI site and the SacII site of the pGEX-hIRF-3 plasmid, respectively. To construct pGEX-hIRF-3ΔC1, the 5925-bp BglII-NotI fragment of pGEX-hIRF-3 was blunt-ended with the Klenow enzyme, and then self-ligated. To construct pGEX-hIRF-3ΔC2 and -ΔC3, the 724-bp NcoI-*Msc*I fragment and the 394-bp NcoI-ScaI fragment were excised from pGEX-hIRF-3 and then subcloned into the blunt-ended NotI site and the NcoI site of the pGEX-hIRF-3 plasmid, respectively. To create a PPIase-defective mutant of CypB, both the arginine at the 96th position and the phenylalanine at the 101st position of CypB were substituted by alanine, using the QuikChange site-directed mutagenesis kit (Stratagene). To construct the Myc-cyclophilin A (CypA) expression plasmid, the CypA cDNA was amplified by RT-PCR using PfuUltra™ DNA polymerase and the gene-specific primers (forward 5′-CGGAATTCGGCACGAGGCCATGGTCAACCCCACC-GTGTTC-3′ and reverse 5′-GCCGCTCGAGTCAAACTTATTCGAGTT-GTCCACAG-3′) with an amplification cycle of 95 °C/30 s, 62 °C/30 s and 72 °C/60 s for 25 cycles. The amplified cDNA was digested with EcoRI and XhoI, and was subcloned into the corresponding sites of pcDNA3-Myc-CypB. *E. coli* strain TG1 was transformed with each plasmid construct, and was grown in LB medium to an $A_{600} > 0.4$. After 3 h of culture in the presence of 2 mM IPTG, for the induction of fusion protein synthesis, the cells were harvested by centrifugation, resuspended in one-twelfth volume of PBS(-) containing 0.5 mM phenylmethylsulfonyl fluoride, and sonicated. The amount of protein used was adjusted on the basis of an SDS-PAGE analysis. The cleared lysates were mixed with 20 μl of glutathione-Sepharose beads for 1 h at 4 °C and subsequently were washed 3 times with DBT-0.1 (dilution buffer with Triton X) (20 mM Hepes-KOH (pH 7.9), 0.5 mM EDTA, 1 mM dithiothreitol, 20% glycerol, 0.2% Triton X-100, 100 mM KCl). The affinity beads were incubated with 150 μl of precleared *in vitro* translated protein for 2 h at 4 °C. After washing the beads 3 times with DBT-0.4 (20 mM Hepes-KOH (pH 7.9), 0.5 mM EDTA, 1 mM dithiothreitol, 20% glycerol, 0.2% Triton X-100, 400 mM KCl), the proteins retained on the beads were extracted in 20 μl of SDS-PAGE sample buffer and were separated on 4–20% SDS gradient gels (Daiichi Chemicals, Tokyo, Japan). Proteins were detected by Western blotting with a rabbit polyclonal anti-Myc antibody (Cell Signaling Technology).

Immunoprecipitation—To detect the association of endogenous IRF-3 and CypB, we performed the immunoprecipitation experiment using the human fibrosarcoma cell line, HT1080. The aliquot of cells was pelleted by centrifugation and infected with NDV for 10 min at 37 °C, and then a whole cell extract was prepared. An aliquot of each extract was incubated with 5 μg of goat IgG or goat polyclonal anti-IRF-3 antibody (C-20, Santa Cruz Biotechnology, Santa Cruz, CA) for 1 h at 4 °C. After this incubation, the protein G beads were added to the mixture and incubated for 4 h at 4 °C. The following procedures were the same as those used for the GST pull-down described above. Proteins were detected by Western blotting with a goat polyclonal anti-IRF-3 antibody (C-20) and a rabbit polyclonal anti-cyclophilin B antibody (Affinity BioReagents. Inc.).

RNA Interference—Human fibrosarcoma HT1080 cells were maintained in Dulbecco's modified Eagle's medium supplemented with 10% fetal bovine serum, 100 μg/ml penicillin, and 50 μg/ml streptomycin in a 37 °C incubator with 5% CO_2 and 100% humidity. The sense and antisense strands of the siRNAs for CypB (5′-GGUGGAGAGCAC-CAAGACATT-3′, 5′-UGUCUUGGUGCUCUCCACCTT-3′) and for the control (5′-ACAGAACCACGAGAGGUGGTT-3′, 5′-CCACCUCU-CGUGGUUCUGUTT-3′) were annealed according to the provider's instructions, respectively (JBioS, Tokyo, Japan). Cells were transfected with siRNAs using Lipofectamine 2000 (Invitrogen). In brief, 1.0 × 10^5 cells/well were seeded in a 6-well tissue culture plate. After 24 h of incubation, the medium was replaced by culture medium without antibiotics. To allow the siRNA-liposome complexes to form, 5 μl of siRNAs (20 μM) and 5 μl of Lipofectamine 2000 reagent were combined in 500 μl of Opti-MEM medium and incubated at room temperature for 20 min. This mixture was added to the cells and incubated for 24 h. The cells were then washed twice with dilution medium (Dulbecco's modified Eagle's medium containing 10% bovine serum albumin) and infected with NDV by the addition of 100 μl of allantoic fluid from NDV-infected chicken eggs (1000 hemagglutinin units/ml) for 1.5 h. After washing twice with complete medium (Dulbecco's modified Eagle's medium supplemented with 10% fetal bovine serum, 100 μg/ml penicillin, and 50 μg/ml streptomycin), the cells were further incubated in complete medium for 10.5 h before harvesting for extract preparation.

Preparation of Whole Cell Extracts—The cells were washed with ice-cold phosphate-buffered saline(−) and then scraped and suspended in 400 μl of cell lysis buffer (50 mM Tris-HCl (pH 8.0), 120 mM NaCl, 0.5% Nonidet P-40, 10% glycerol, 2 mM Na_3VO_4, 10 mM NaF, 0.2 mM phenylmethylsulfonyl fluoride). The cells were lysed by vortexing briefly, and the lysates were incubated on ice for 10 min. The whole cell extracts were recovered after centrifugation at 15,000 rpm for 10 min at 4 °C.

Western Blotting—The procedures were the same as those used in the GST pull-down experiment described above. The antibodies used were the goat polyclonal anti-IRF-3 antibody (C-20), the mouse monoclonal anti-IRF-3 Ser(P)-396 antibody (HIS5133, a gift provided by Drs. J. Hiscott and M. Servant, McGill University), the rabbit polyclonal anti-cyclophilin B antibody, and the mouse monoclonal anti-actin antibody (Chemicon).

Native PAGE Assay—The native PAGE assay was performed by using 7.5% polyacrylamide gels (Daiichi Chemicals). The gel was prerun in a running buffer containing 25 mM Tris and 192 mM glycine, with and without 1% deoxycholate in the cathode and anode chambers, respectively, for 30 min at 40 mA. Aliquots of whole cell extracts were diluted in native sample buffer (62.5 mM Tris-HCl (pH 6.8), 15% glycerol, and 1% deoxycholate), applied to the gel, and electrophoresed for 60 min at 25 mA. Immunoblotting was performed as described above. Proteins were detected by Western blotting with a goat polyclonal anti-IRF-3 antibody (C-20) or a rabbit polyclonal anti-IRF-3 Ser(P)386 antibody (IBL).

Electrophoretic Mobility Shift Assay—To examine the binding of IRF-3 to the IFN-β promotor, an electrophoretic mobility shift assay was performed using whole cell extracts from siRNA-transfected and NDV-infected or -uninfected HT1080 cells. The extracts were incubated in a reaction buffer (25 mM Tris-HCl (pH 8.0), 60 mM NaCl, 0.25% Nonidet P-40, 5% glycerol, 1 mM Na_3VO_4, 5 mM NaF, 1 mM dithiothreitol, 100 mg/ml poly(dI-dC)). After a 30-min incubation on ice, ~10,000 cpm of a ^{32}P-labeled double-stranded oligonucleotide containing the ISRE sequence of the ISG15 gene (5′-GGGAAAGGGAAACCGAAACT-GAA-3′) were added to the reactions, which were then incubated for an additional 30 min at 25 °C. The reactions were further incubated with an anti-IRF-3 antibody (C-20) or an anti-CBP antibody (A-22X) (Santa Cruz Biotechnology) for 30 min at 25 °C. The binding reactions were mixed with 1 μl of loading buffer (0.1% bromphenol blue in the same buffer used for the binding reactions) and then were electrophoresed on a nondenaturing 4% polyacrylamide gel with 0.5 × TBE (Tris borate-EDTA) at 200 V for 2 h. The gel was dried and analyzed by an image analyzer, BAS5000 (Fuji, Tokyo).

Chromatin Immunoprecipitation Assay—HT1080 cells were mock- or NDV-infected for 12 h and then treated with formaldehyde to cross-link the proteins bound to DNA. The cross-linked proteins were purified and immunoprecipitated with the anti-IRF-3 antibody (C-20). After reversal of the cross-linking, the DNA was amplified using primers for the ISG15 promoter (5′-TTTTCCCTGTCTTTCGGTCATTCG-3′, 5′-TAT-TATAAGCCTGAGGCACACACG-3′) with an amplification cycle of 94 °C/1 min, 55 °C/1 min, and 72 °C/2 min for 30 cycles.

Enzyme-linked Immunosorbent Assay for IFN-β—The amounts of human IFN-β in the culture medium supernatants before and after NDV infection were quantified with a human interferon-β enzyme-linked immunosorbent assay kit (R&D Systems). Data are expressed as the mean ± S.D. Differences among groups were examined for statistical significance using one-factor analysis of variance (Bonferroni/Dunn). A p value < 0.05 denoted the presence of a statistically significant difference.

RESULTS

Isolation of Putative IRF-3-binding Proteins by the Bacterial Two-hybrid Screening—To isolate the protein(s) that associate with IRF-3, we performed a screening by a bacterial two-hybrid system (16, 17). The bait was fused to the full-length bacteriophage λ repressor protein (λ*cI*), whereas the corresponding target protein was fused to the N-terminal domain of the α-subunit of RNA polymerase. When the bait and target interact, they recruit and stabilize the binding of RNA polymerase at the promoter and activate the transcription of reporter genes, the carbenicillin-resistance and the β-galactosidase genes. In addition, this system offers the ability to detect an interaction between a pair of protein domains with an equilibrium dissociation constant in the high nanomolar range. In the present study, we used IRF-3 as the bait and a human HeLa cell cDNA library as the target. We obtained 272 antibiotic-resistant and *lac*Z-positive clones from 4.30×10^6 screened clones. To identify the protein encoded by the candidate positive clones, the nucleotide sequence of each clone was determined. Among the clones obtained, only 25 clones encoded in-frame fusion proteins to the λ*cI* repressor. These clones were used in a search for homology in the NCBI data base. The cDNA fragments of the positive clones were subcloned into an expression vector to produce N-terminally Myc-tagged fusion proteins. However, we obtained *in vitro* coupled transcription/translation products from only 13 of 25 clones. For these 13 clones, we performed a GST pull-down assay to confirm their binding activities to IRF-3. Only clone A25 (cyclophilin B) showed specific binding to IRF-3 (data not shown). Therefore, we concentrated our efforts on the interaction between IRF-3 and CypB.

Mapping the IRF-3 and Cyclophilin B Interaction Domains—To confirm the specificity of the interaction between IRF-3 and CypB, we examined which region of IRF-3 is important for binding to CypB. A GST pull-down assay was performed with a series of IRF-3 deletion mutants fused to GST and *in vitro* translated full-length CypB (Fig. 1*A*). As mentioned above, CypB bound to GST-IRF-3 but not to GST alone (Fig. 1*B*, *lanes 3* and *2*). The deletion of the N-terminal DNA-binding domain somehow enhanced the binding of CypB (Fig. 1*B*, *lane 4*), whereas further removal of the nuclear export signal and the proline-rich region reduced the affinity to CypB (*lane 5*). Unexpectedly, the deletion of the IAD restored the interaction potential of IRF-3 to CypB (Fig. 1*B*, *lane 6*). When we removed the C-terminal 296 residues from IRF-3, the interaction with CypB was not detected (Fig. 1*B*, *lane 9*). It is noteworthy that the mutants ΔN3 and ΔC1 do not share any regions of IRF-3 but still exhibited the CypB binding, suggesting that IRF-3 has multiple sites for CypB binding. Furthermore, the IAD seems to have an inhibitory effect on the binding, as the binding of ΔN2 is weaker than that of ΔN3, the construct lacking two thirds of the IAD from ΔN2. We did not perform a GST pull-down analysis with GST-CypB to detect the binding with IRF-3, because the GST-CypB expression plasmid failed to produce a detection level of the protein in *E. coli*.

Next, we examined the regions of CypB required for the interaction with IRF-3. Because CypB is a rather small protein (208 amino acids), even a small deletion drastically destabilized the mutant forms of the protein (data not shown). Thus, we tested whether the PPIase activity of CypB, a well known biological activity of the protein, was required for the binding to IRF-3. For this purpose, arginine 96 and phenylalanine 101 in the PPIase domain of CypB were substituted with alanines by site-directed mutagenesis (Fig. 1*C*). As shown in Fig. 1*D*, the PPIase mutant did not bind to IRF-3 (*lane 9*). In addition, we found that cyclophilin A (CypA), the most abundant cyclophilin *in vivo*, could not bind to IRF-3 (*lane 3*).

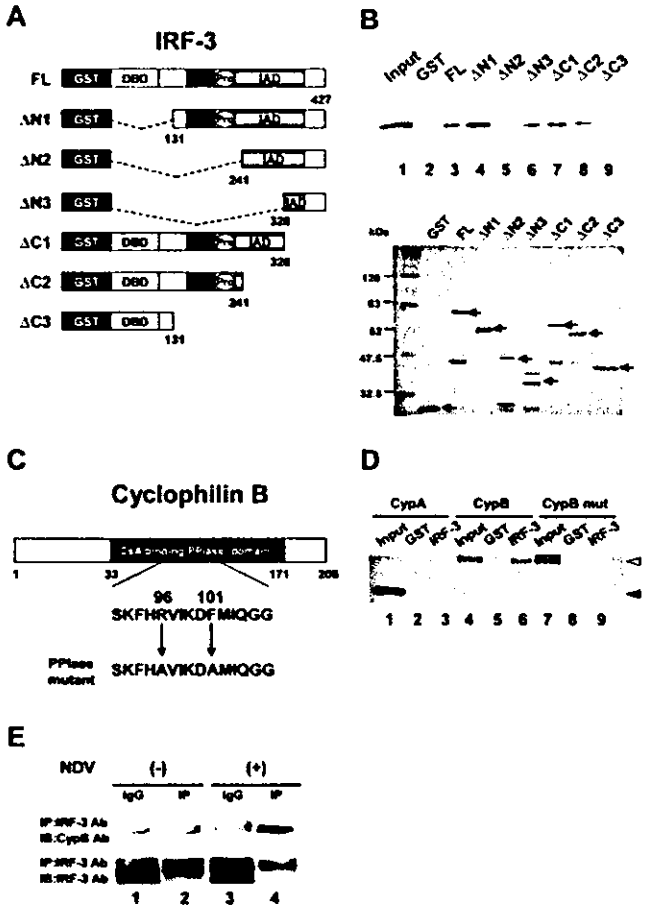

FIG. 1. **Mapping the interaction domains of IRF-3 and CypB.** *A*, schematic representation of IRF-3 deletion mutants. Structures of wild type (*top*) and deletion mutants (ΔN1–3 and ΔC1–3) of IRF-3 are shown. Locations of functional domains are indicated. *DBD*, DNA-binding domain; *NES*, nuclear export signal; *Pro*, proline-rich region; *IAD*, interferon-associated domain. *B*, GST pull-down assay between IRF-3 mutants and CypB. *Input*, 5% of *in vitro* translated Myc-tagged CypB was included in the binding reactions. *GST*, GST protein only (not fused with IRF-3); *FL*, GST fusion of wild type IRF-3 protein; *ΔN1*, GST fusion of IRF-3 truncated 131 residues from the N terminus; *ΔN2*, GST fusion of IRF-3 truncated 241 residues from the N terminus; *ΔN3*, GST fusion of IRF-3 truncated 328 residues from the N terminus; *ΔC1*, GST fusion of IRF-3 truncated 99 residues from the C terminus; *ΔC2*, GST fusion of IRF-3 truncated 186 residues from the C terminus; *ΔC3*, GST fusion of IRF-3 truncated 296 residues from the C terminus. *C*, schematic representation of cyclophilin B PPIase mutants. The wild type CypB structure (*top*) is shown. The amino acid sequence of the wild type CypB and the mutated residues are shown. *CsA*, Cyclosporin A. *D*, GST pull-down assay between CypB, CypB PPIase mutant, or CypA and wild type IRF-3. *Input*, 5% of *in vitro* translated Myc-tagged CypB, Myc-tagged CypB PPIase mutant, or Myc-tagged CypA was included in the binding reactions, respectively. *GST*, GST protein only (not fused with IRF-3); *IRF-3*, GST-fusion of wild type IRF-3 protein. The *solid* and *empty arrowheads* indicate CypB and CypA, respectively. *E*, co-immunoprecipitation assay to detect an endogenous association between IRF-3 and CypB *in vivo*. Whole cell lysates prepared from cells, either mock-infected or NDV-infected for 10 min, were used as the input. *IgG*, lysates incubated with goat IgG (*lanes 1* and *3*) *IP*, lysates incubated with goat polyclonal anti-IRF-3 antibody (C-20) (*lanes 2* and *4*). *IB*, immunoblot. The data are representative of three independent experiments.

Then, we examined the interaction between IRF-3 and CypB *in vivo*. The association of endogenous IRF-3 and CypB was detected when an anti-IRF-3 antibody was used for the precipitation of an extract prepared 10 min after NDV infection (Fig. 1*E*, *lane 4*) but not 30 min after the infection (data not shown). On the other hand, the available anti-CypB antibodies could